

STUDY OF SUBMERGED AIR JETS IN LIQUIDS

By

ASHFAQ MOHAMMAD ANSERY

A THESIS

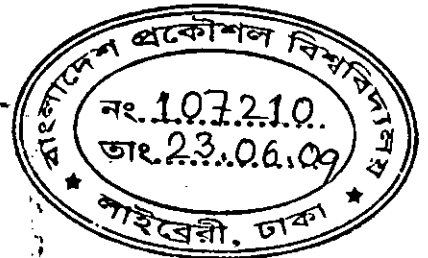
SUBMITTED TO THE DEPARTMENT OF CHEMICAL ENGINEERING IN
PARTIAL FULFILLMENT OF THE REQUIREMENTS FOR THE DEGREE
OF
MASTER OF SCIENCE IN CHEMICAL ENGINEERING

DEPARTMENT OF CHEMICAL ENGINEERING
BANGLADESH UNIVERSITY OF ENGINEERING AND TECHNOLOGY
DHAKA-1000, BANGLADESH

April 2009



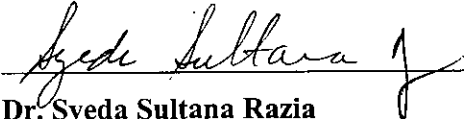
#107210#



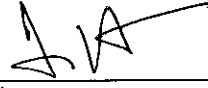
RECOMMENDATION OF THE BOARD OF EXAMINERS

The board of examiners hereby recommends to the Department of Chemical Engineering, BUET, Dhaka, the acceptance of this thesis titled, "STUDY OF AIR JET STABILITY IN LIQUIDS" submitted by **Ashfaq Mohammad Ansery**, Roll No: **040502008P**, Session: **April 2005**, as satisfactory in partial fulfillment of the requirements for the degree of Master of Science in Chemical Engineering on April 6, 2009.

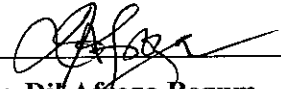
Chairman (Supervisor):


Dr. Syeda Sultana Razia
Associate Professor
Department of Chemical Engineering
BUET, Dhaka-1000, Bangladesh

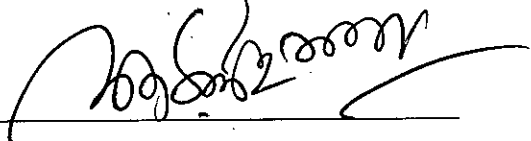
Member (Ex-officio):


Dr. Ijaz Hossain
Professor & Head
Department of Chemical Engineering
BUET, Dhaka-1000, Bangladesh

Member:


Dr. Dil Afroza Begum
Professor
Department of Chemical Engineering
BUET, Dhaka-1000, Bangladesh

Member (External):


Dr. A.K.M. Sadrul Islam
Professor
Department of Mechanical and
Chemical Engineering
Islamic University of Technology, Bangladesh

CERTIFICATE OF RESEARCH

This is to certify that the work presented in this thesis is carried out by the author under the supervision of Dr. Syeda Sultana Razia, Associate Professor, Department of Chemical Engineering, Bangladesh University of Engineering & Technology, Dhaka-1000, Bangladesh.

Dr. Syeda Sultana Razia

Ansery

Ashfaq M Ansery

Ashfaq Mohammad

DECLARATION

No portion of the work contained in this thesis has been submitted in support of an application for another degree or qualification of this or any other University or Institution of learning.

Ashfaq M Ansery

Ashfaq Mohammad Ansery

Author

Dedicated to my mother

ACKNOWLEDGEMENT

I am indebted to many individuals who have supplied information and comments on the materials presented in this thesis paper. I acknowledge all those who provided untiring cooperation for successful completion of this research project. My sincere apology goes out to those names that I have mistakenly omitted here.

First of all, I gratefully acknowledge the contributions of Dr. Syeda Sultana Razia, Associate Professor, Department of Chemical Engineering, Bangladesh University of Engineering and Technology (BUET), who as my thesis supervisor provided a motivating, enthusiastic, and critical atmosphere during the many discussions we had. It was an immense pleasure to me to have an opportunity to conduct this thesis project under her supervision. It was her valuable and constructive ideas, comments and useful suggestions during the time of this thesis project that have manifested numerous improvements in my research work. The experience of working under her supervision is one that I will cherish long after this thesis is completed.

I am deeply indebted to Dr. Muhammed Mahbubur Razzaque, Associate Professor, Department of Mechanical Engineering, BUET for his generous and effective suggestions and continuous assistance in all possible ways especially to formulate the experimental set-up, to understand the critical features of light and camera projection and to install U-Lead Studio for collection and treatment of data.

I also express my sincere gratitude Dr. M. Sadrul Islam, Professor, Department of Mechanical Engineering, Islamic University of Technology, Bangladesh and Dr. Dil Afroza Begum, Professor, Chemical Engineering Department, BUET who shed some useful insight into my thesis project and make useful suggestions. I greatly owe to Dr. M.A.A. Shoukhat Choudhury for giving me the easy access and assistance to use his online library.

I acknowledge my gratitude to Dr. Ijaz Hossain, Professor & Head, Chemical Engineering Department, BUET for his commitment of the resources of the department to the accomplishment of this important task.

I like to thank the entire staff of the Chemical Engineering Department office, library, Unit Operation laboratory, specially, technician Mr. Mahbub and Mr. Jahangir who generously helped me during my laboratory work. They have extended all out support to my experimental work even at the expense of some of their weekends.

Last, but far from least is my wife, Selina, who suffered so much but never lack the motivation and inspiration for me. Without her steadfast devotion and support, successful completion of this research project would not have been possible.

ABSTRACT

Submerged gas injection has attracted much attention due to its wide range of application in different processes. A number of numerical analysis has been made to investigate the stability of submerged air jet in liquids. Experimental studies are however scarce. In present study for the first time a systematic experimental study of submerged gas jet is made. Experimental investigation on submerged air jet was carried out in a $14 \times 14 \text{ cm}^2$ Perspex column with a liquid height of 25 cm. The jets were generated by flowing air at different velocities through nozzles immersed at the bottom of a stagnant liquid column. The diameters of the nozzles used were 1, 4 and 6 mm. The jet formation was observed in three different liquids, namely, water, ethanol and glycerol. The minimum jet formation velocity was recorded and jet lengths at different velocities were measured by image processing. The data showed that the jet length increases as the velocity increases until it reaches a maximum value. Beyond this value, the jet length decreases as the velocity increases. The jet formation velocities as well as the jet lengths for all three gas/liquid systems are increased with decreasing nozzle diameter. Viscosity of the liquid was found to have a destabilizing effect on jet break-up length. The observed phenomena are explained with the aid of instability theory and compared with existing theoretical analysis.

NOMENCLATURE

Symbol	Definition
a	radial length
B_1, B_2 and B_3	dimensionless ratios of Bessel functions
D	diameter of the nozzle
g	gravitational acceleration
H, L	height or length of the jet
L_{\max}	Maximum jet length
M	Mach number
Re	Reynolds number
T, t	Time
U, u	velocity of jet
$U_{L_{\max}}$	Maximum velocity of jet
U_c	sonic velocity
We	Weber number

Greek Symbols

α	growth rate
$\alpha_{L_{\max}}$	growth rate of disturbance at L_{\max}
α_r	time amplification factor of the disturbance
α_i	angular frequency of the disturbance
η	disturbance
η_0	initial disturbance
κ	wave number
λ	wavelength
μ_G, μ_L	viscosity of gas and liquid

ρ_G, ρ_L density of liquid and gas
 σ surface tension

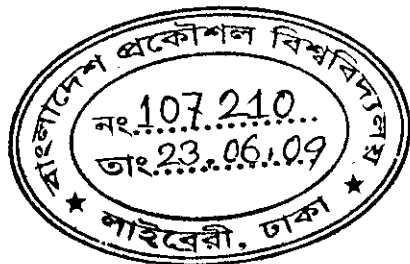
Subscript

G Gas

L Liquid

CONTENTS

RECOMMENDATION OF THE BOARD OF EXAMINERS	i
CERTIFICATE OF RESEARCH	iii
DECLARATION	iv
ACKNOWLEDGEMENT	vi
ABSTRACT	viii
NOMENCLATURE	ix
CONTENTS	xi
Chapter 1 Introduction	1
Chapter 2 Literature Review	4
2.1 Experimental and Theoretical Stability Investigations of Liquid Jets	4
2.2 Instability Analysis of the Liquid-Gas Interface of Submerged Gas Jets	14
2.3 The Effect of Mass Transfer on the Instability of Interface of Gas Jet Submerged in a Liquid	18
2.4 Experimental Analysis of Liquid-Gas Interface at Low Weber Number	20
2.5 Experimental Study on Hydrodynamic Behaviours of High-Speed Gas Jets in Still Water	22
Chapter 3 Theoretical Development	25
Chapter 4 Experimental	28
Chapter 5 Results and Discussion	34
5.1 Effect of Nozzle Size	37
5.2 Effect of Liquid Properties	39
5.3 Effect of Jet Velocity	40
Chapter 6 Conclusion	45
Chapter 7 Reference	46
Appendix A Physical Properties of Liquids	51
Appendix B Data Obtained for Air/Liquid System at Various Nozzle Size	52
Appendix C Different Plots for Air/Liquid System at Various Nozzle Size	65



Chapter 1 Introduction

Free liquid jet flow has attracted much attention since the beginning of the last century due to its wide range of industrial applications, e.g. jet cutting, fuel injection and cooling through impingement. Like liquid jet, submerged gas injection into liquids has also got important applications in different processes such as in metallurgical processes, which involve high temperatures. Submerged bubbling/jetting is employed to enhance heat and mass transfer rates to produce large interfacial areas. Submerged turbulent gas jets are of particular interest in a number of applications; such as in stored chemical energy propulsion systems for underwater applications, in basic oxygen steel making processes; in steam generator safety analysis (steam jets submerged in liquid sodium) of liquid metal-cooled reactors etc. Prediction of design parameters of such equipment largely depends on the jet length. The research has historically been focused on the flow and break-up of cylindrical liquid jets in order to predict and control droplet size.

For submerged liquid jets research started in the middle of the last century whereafter it gradually increased due to its industrial importance. As one of the earliest results using linear stability theory by Rayleigh [1] considered a liquid jet with a uniform velocity distribution, i.e. the flow is parallel and the velocity constant throughout the jet. Viscosity in the liquid was neglected, i.e. the flow was assumed to be inviscid and the effect of the ambient gas was neglected. Superficial forces were assumed to act on the surface of the jet and the analysis was performed by making an assumption of infinitesimal perturbation acting on the surface of the jet. This gave as result a prediction of a growth or decay of the disturbances on the jet. The result showed that growth only could be obtained for axisymmetric disturbances with a wavelength λ that satisfies $\lambda > 2\pi a$, where "a" is the radius of the cylinder.

Later linear stability theory has been used extensively for various flow situations [2]. For the break-up of a cylindrical liquid jet the original approach by Rayleigh has been extended to include viscosity and non-linear effects. Investigations have been done both experimentally and numerically and a comprehensive investigation of low-speed jet behavior in liquid/liquid system was made by Grant and Middleman [3]. They reported the results in the form of break-up curves. It was observed that that jet break-up length increases linearly with increasing jet velocity. Thereafter it reaches a maximum and then decreases. Most of these experimental studies are, however, confined to liquid/liquid systems.

For gas/liquid system a number of theoretical studies are available in literature. Korja [4] presented a simple structure model and calculated the non-buoyant jet length of gas jets in a metal bath. He concluded that for injection velocities of Mach number <1 , the gas jet disintegrates in the form of bubbles very close to the gas injecting orifice, and a bubble column forms in the metal bath. For Mach number >1 , the length of the non-buoyant jet in the bath is appreciable and the jet disintegrates later into bubbles. Chawla [5] included a non-zero wave velocity in his study of the stability of a sonic gas jet submerged in liquid. However his numerical result pertains only to a Mach number of unity. Chan et al. [6] extended this study of sonic jet to include the effect of mass transfer on the Kelvin-Helmholtz instability of the gas-liquid interface. Chen and Richter [7] developed a basic theory to explain the transition from bubbling to jetting. The instability of a circular compressible gas jet in a liquid was studied. For the axisymmetric mode, it was found that there is a peak growth rate for both the temporal and spatial instabilities when the Mach number approaches unity. Gas pressure perturbations have a destabilizing effect in the subsonic region but a stabilizing effect in the supersonic region. The problem of absolute instability was studied by Chen and Richter [7] in order to explain the physical phenomenon of the transition from bubbling to jetting. Absolute instability was found in the subsonic region and a gas jet always breaks up into bubbles in the subsonic region. No absolute instability was found in the supersonic region, and the gas jet may remain stable. This transition from absolute to non-absolute instability occurs in the transonic region which was observed to be the transition from bubbling to jetting.

Although considerable works have been devoted to theoretical study of gas jet stability in liquids, experimental investigations to validate these theories are scarce. No comprehensive study on jet formation and jet disintegration, particularly on the variation of jet length with geometry and physical properties is available in existing literature.

The present study dealt with experimental study of submerged air jets and interpreting the jet behavior with the help of existing theoretical understanding of stability of submerged jets. The objectives of this project are to measure the length of the air jet submerged in liquids under different flow condition at various nozzle sizes and to understand the effect of interfacial disturbance in jet-breakup process/mechanism by comparing the experimental findings with the numerical analysis reported in the literature.

Chapter 2

Literature Review

Jet is one of the most common flow configurations that are encountered both in nature and industrial applications frequently. Considering the significant use and occasions of jets, lots of research works have been done in the past and still are going on at present on stability of jets both for liquid/liquid and gas/liquid system. The reviews of some of the earlier research works related to the present investigation are presented below:

2.1 Experimental and Theoretical Stability Investigations of Liquid Jets

Free liquid jet flow has attracted much attention during the history of fluid mechanics and is used in many industrial applications, e.g. jet cutting, fuel injection and cooling through impingement. The research has historically been focused on the flow and break-up of cylindrical liquid jets in order to predict and control droplet size. For plane liquid jets research started in the middle of this century whereafter it gradually increased due to its industrial importance.

The stability analysis of liquid jets is relevant for the analysis of several commercial atomization devices and, in particular, for pressure atomizers such as those used in diesel engines, turbojet afterburners, ink-jet printers, etc.

Break-up of a liquid jet into droplets has been involved in many practical applications such as in diesel engines, gas turbine engines, liquid rocket engines, oil burners, spray coating process, plastics manufacture, metal powder production, lubrication, and so on. Therefore, it is of interest and importance to understand the mechanisms of instability and break-up of liquid jets, since the efficiency and quality of production is strongly dependent on these mechanisms.

Gas-liquid jet reactors are widely used in commercial applications such as condensing jets for direct contact feedwater heaters and steam jet pumps, because of their efficient heat- and mass-transfer characteristics. These are also used for the blowdown of primary nuclear boiler systems into a water bath, without releasing fissionable materials into the atmosphere. Reacting jets are of major interest in metal processing and thermal energy sources that involve submerged injection of an oxidizer into a liquid metal bath.

Initially, Rayleigh [1] considered an inviscid liquid jet with uniform velocity distribution. Superficial forces were assumed to act on the surface of the jet and the analysis was performed by making an assumption of infinitesimal perturbation acting on the surface of the jet. The result showed that growth only could be obtained for axisymmetric disturbances with a wavelength λ that satisfies $\lambda > 2\pi a$, where "a" is the radius of the cylinder.

Later linear stability theory has been used extensively for various flow situations [2]. For the break-up of a cylindrical liquid jet the original approach by Rayleigh has been extended to include viscosity and non-linear effects. Investigations have been done both experimentally and numerically and are reviewed by McCarthy and Molloy [8] and Bogy [9]. It has been shown that stability of liquid jets depends largely on fluid properties, turbulence, nozzle size etc. Experimentally, Goedde and Yuen [10] showed that non-linear effects cause ligaments between drops when the jet disintegrates. Also, it can be shown that the flow of a cylindrical liquid jet can be globally unstable, if proper boundary conditions are imposed at the upstream and downstream boundaries [11].

The effect of a non-uniform velocity distribution inside a cylindrical jet has also been considered, theoretically by Leib and Goldstein [12] and experimentally by Debler and Yu [13]. The theoretical result was based on a spatial stability analysis and the conclusion is that the growth of a disturbance is reduced when the velocity profile in the liquid jet deviates from the uniform. The experiments by Debler and Yu [13], were carried out by investigating the stability of a circular liquid jet emanating from

tubes of varying length. With a constant flow rate through the tubes the profiles at the end of the tubes are more or less developed. The experiments gave qualitatively the same result as the theory, i.e. the growth rate is reduced with a non-uniform profile. The experiments also showed a significant effect of the upstream conditions on the break-up length of the jet. A higher turbulence level gave a more rapid disintegration of the jet. These investigations were all aimed at the break-up into discrete droplets by axisymmetric disturbances.

If the velocity of the jet is increased the break-up will be different [14]. They made visualisations of a circular liquid jet emanating from a converging nozzle which ended in a short straight pipe. The experiment also allowed for a co-flowing gas which could have a higher velocity than the liquid in the jet. Close to the exit short waves, i.e. their wavelength was much shorter than the jet diameter, could be seen. These waves were observed to break up a few jet diameters downstream the exit. The result of the break-up was formation of spray droplets, and the break-up was not sensitive to the velocity of the ambient gas. Further downstream a helical disturbance could be seen growing. This disturbance had large amplitude and was enhanced by a higher velocity of the gas. The wavelength of the short waves was compared with linear stability results by Brennen [15], which were obtained for a hydrodynamic cavity behind an axisymmetric body.

If the liquid jet emanates from a sufficiently long channel it will have a parabolic velocity distribution in the end of the channel, This profile will relax due to the change in boundary condition and somewhere downstream the velocity distribution will be uniform. This case was studied by Hashimoto and Suzuki [16] experimentally and theoretically. By visualisations they found fine interfacial waves close to the nozzle which were explained by linear stability theory. A shooting method was used to solve the linear stability problem and this gave four unstable modes, two even and two odd. The first pair of these modes was called soft modes and the second pair were named hard modes. The hard modes had growth rates which were considerably higher when compared to the maximum growth rate for the first pair. The velocity profiles

used in their stability calculations were taken from Lienhard [17] and the effect of an ambient gas was not considered.

A high-velocity jet of a given liquid discharges from a circular hole into a stagnant atmosphere, and different breakup regimes present themselves depending on a large number of parameters, such as liquid-jet velocity, nozzle design and gas density. The injector geometry influences the liquid-jet breakup; as pointed out by Reitz & Bracco [18] and Lin & Reitz [19], turbulence, liquid velocity profile and cavitation within the nozzle are factors which can decisively affect the breakup of the liquid jet. On the other hand, with regard to the outer atmosphere influence on the jet breakup, Reitz & Bracco [18] concluded that if the outer gas density is increased and both the nozzle geometry and the liquid injection velocity are kept constant, the growth rate of perturbations leading to the jet breakup is enhanced.

Under these conditions, it is experimentally observed that, for the lower injection velocities, a liquid jet is not formed and a dripping regime is obtained owing to surface-tension confinement forces overcoming liquid inertia and gravity. If the liquid velocity is progressively increased by keeping the rest of parameters constant, a liquid jet is formed giving rise to a jetting regime. For the lower liquid velocities within the jetting regime, the breakup length l_b depends linearly on the injection velocity U_L . This can be explained by Rayleigh's [50] pioneering investigations. In Rayleigh's analysis, the inertia of the outer atmosphere is not taken into account and, therefore, surface-tension forces are the only ones responsible for instability. However, for a larger injection velocity, we obtain the so-called *first wind-induced breakup regime* (FWI), for which experiments show that the liquid jet length increases with velocity until it reaches a maximum [19,20]. In these experiments, the shortening in the breakup length that can be solely attributed to aerodynamic effects due to l_b is such that $l_r \ll l_b$ where l_r is the liquid relaxation length and U_L and ν_L are the liquid injection velocity and kinematic viscosity, respectively. The size of the drops in the FWI is still of the order of the jet radius, although smaller than those obtained in the Rayleigh regime.

In spite of all the experimental and theoretical efforts made through the years, Rayleigh's breakup regime is the only one that is perfectly understood. In an attempt to explain the experimental results at larger injection velocities, Weber [21] extended Rayleigh's work to include the effect of the surrounding gas inertia into the stability analysis. Weber considered a simple Kelvin-Helmholtz model, uniform liquid and gas velocity profiles, and retained viscosity only in the liquid linear stability equations. He found that the inclusion of aerodynamic effects into the analysis predicts, as observed experimentally, a maximum in the curve of breakup length vs. injection velocity.

However, the maximum predicted by Rayleigh [1] and Weber [21] occurs for lower velocities than those measured experimentally, which led Sterling & Sleicher [20] to extend the analysis by including the effect of the gas viscosity. For this purpose, they introduced an ad hoc parameter whose effect is to reduce the perturbed gas pressure at the jet interface. The value of this parameter (0.175) was adjusted so that the predicted break-up lengths agreed with the experimental ones. The good agreement with the experiments suggests that the Sterling & Sleicher [20] approximation to account for gas viscosity is conceptually valid. However, in spite of the importance of the FWI breakup regime for numerous applications, there is still no study in the literature that includes, self-consistently, the effect of gas viscosity in the equations governing the liquid-jet breakup.

J. M. Gordillo and M. Perez-Saborid [22] presented both numerical and analytical results from a spatial stability analysis of the coupled gas-liquid hydrodynamic equations governing the first wind-induced (FWI) liquid-jet break-up regime. Their study shows that an accurate evaluation of the growth rate of instabilities developing in a liquid jet discharging into a still gaseous atmosphere requires gas viscosity to be included in the stability equations even for low We_G , where $We_G = \rho_g U_L^2 R_0 / \sigma$, and ρ_g , U_L , R_0 and σ are the gas density, the liquid injection velocity, the jet radius and the surface tension coefficient, respectively. The numerical results of the complete set of equations, in which the effect of viscosity in the gas perturbations is treated self-consistently for the first time, are in accordance with recently reported experimental

growth rates. This permits us to conclude that the simple stability analysis presented here can be used to predict experimental results.

Moreover, in order to throw light on the physical role played by the gas viscosity in the liquid-jet break-up process, J. M. Gordillo and M. Perez-Saborid [22] have considered the limiting case of very high Reynolds numbers and performed an asymptotic analysis which provides us with a parameter, α , that measures the relative importance of viscous effects in the gas perturbations. The criterion $|\alpha| \ll 1$, with α computed a priori using only the much simpler inviscid stability results is a guide to assess the accuracy of a stability analysis in which viscous diffusion is neglected. J. M. Gordillo and M. Perez-Saborid [22] have also been able to explain the origin of the ad hoc constant 0.175 introduced by Sterling & Sleicher [20] to correct the discrepancies between Weber's results.

Reitz and Bracco [18] considered the break-up of a high-speed liquid jet injected through a circular nozzle into an initially stagnant gas. Under appropriate conditions a diverging conical spray is produced which contains droplets of size much less than the nozzle exit diameter. The point where the divergence of the jet begins depends on the conditions. The regime of interest in this work is that in which the divergence begins at the nozzle exit and Reitz and Bracco [18] called this class of jet breakup atomization. It should be noted that there appears to be no generally accepted definition of the term atomization.

In spite of the importance of atomization in applications, the mechanism by which atomization occurs is still not well understood. In contrast, the theoretical understanding of the controlling process for the breakup of low-speed jets has been developed well. Indeed, for high-speed atomizing jets, conflicting theories have been proposed over the years which still remain largely untested. Thus, the atomization mechanism have been ascribed to aerodynamic interaction effects, liquid turbulence, jet velocity profile rearrangement effects, cavitation phenomena, and liquid supply pressure oscillation by various authors. In this study Reitz and Bracco [40] examined

the validity of these and other proposed mechanisms for atomization with the help of experiments.

In the atomization regime of a round liquid jet, a diverging spray is observed immediately at the nozzle exit. The mechanism that controls atomization has not yet been determined even though several have been proposed. Experiments are reported with constant liquid pressures from 500 psia (33 atm) to 2500 psia (166 atm) with five different mixtures of water and glycerol into nitrogen, helium, and xenon with gas pressures up to 600 psia (40 atm) at room temperature. Fourteen nozzles were used with length-to-diameter ratios ranging from 85 to 0.5 with sharp and rounded inlets, each with an exit diameter of about 340 μm . An evaluation of proposed jet atomization theories shows that aerodynamic effects, liquid turbulence, jet velocity profile rearrangement effects, and liquid supply pressure oscillations each cannot alone explain the experimental results. However, a mechanism that combines liquid-gas aerodynamic interaction with nozzle geometry effects would be compatible with our measurements but the specific process by which the nozzle geometry influences atomization remains to be identified.

The conclusions of this study, in general, and those about the mechanism of atomization, in particular, were obtained by varying the liquid pressure and viscosity, the gas pressure and density, and the nozzle geometry within specified ranges. Outside of these ranges, additional breakup mechanisms are known to exist. Moreover, the nozzle exit diameter, the liquid density and surface tension, and the gas and liquid temperatures were not varied significantly. Their variation may necessitate consideration of other effects in the atomization mechanism. Indeed, had the nozzle geometry not been varied in the present study, one could have concluded that the aerodynamic surface wave growth mechanism, alone, was fully able to explain the experimental results.

The temporal instability behaviour of a viscoelastic liquid jet in the wind-induced regime with axisymmetric and asymmetric disturbances moving in an inviscid gaseous environment is investigated theoretically. The corresponding dispersion

relation between the wave growth rate and the wavenumber is derived. The linear instability analysis shows that viscoelastic liquid jets are more unstable than their Newtonian counterparts, and less unstable than their inviscid counterparts, for both axisymmetric and asymmetric disturbances, respectively. The instability behaviour of viscoelastic jets is influenced by the interaction of liquid viscosity and elasticity, in which the viscosity tends to dampen the instability, whereas the elasticity results in an enhancement of instability. Relatively, the effect of the ratio of deformation retardation to stress relaxation time on the instability of viscoelastic jets is weak. It is found that the liquid Weber number is a key measure that controls the viscoelastic jet instability behaviour. At small Weber number, the axisymmetric disturbance dominates the instability of viscoelastic jets, i.e., the growth rate of an axisymmetric disturbance exceeds that of asymmetric disturbances. When the Weber number increases, both the growth rate and the instability range of disturbances increase drastically. The asymptotic analysis shows that at large Weber number, more asymmetric disturbance modes become unstable, and the growth rate of each asymmetric disturbance mode approaches that of the axisymmetric disturbance. Therefore, the asymmetric disturbances are more dangerous than that of axisymmetric disturbances for a viscoelastic jet at large Weber numbers. Similar to the liquid Weber number, the ratio of gas to liquid density is another key measure that affects the viscoelastic jet instability behaviour substantially.

Zhihao Liu and Zhengbai Liu [23] showed that the temporal instability behaviour of a viscoelastic liquid jet in the wind-induced regime with axisymmetric and asymmetric disturbances moving in an inviscid gaseous environment is investigated theoretically. As a result of the linear analysis described above, the following conclusions may be drawn.

In the investigated regime, the growth rate of wave on a viscoelastic liquid jet is larger than that of a Newtonian one and smaller than that of an inviscid one for axisymmetric disturbance, and for each asymmetric disturbance mode, this same phenomenon holds true, i.e., this phenomenon is independent of the values of n , indicating that viscoelastic liquid jets are more unstable than their Newtonian

counterparts, and less unstable than their inviscid counterparts for both axisymmetric and asymmetric disturbances.

The liquid Weber number is a key measure that controls the viscoelastic jet instability behaviour. At small Weber number, the axisymmetric disturbance dominates the instability of viscoelastic jets, i.e., the growth rate of an axisymmetric disturbance exceeds that of the asymmetric disturbances and the growth rate of asymmetric disturbances decreases as the value of n increases. When the Weber number increases, both the growth rate and the instability range of disturbances increase drastically. The asymptotic analysis shows that at large liquid Weber number, more asymmetric disturbance modes with large values of n become unstable, and the growth rate of each asymmetric disturbance mode approaches that of the axisymmetric disturbance in most of disturbance range. In addition, at small wavenumber, the growth rate of the sinuous disturbances ($n = 1$) is greater than that of the varicose disturbances ($n = 0$). Therefore, the asymmetric disturbances are more dangerous than that of the axisymmetric disturbance for viscoelastic jets at large Weber numbers.

Similar to the liquid Weber number, the ratio of gas to liquid density is another key measure that controls the viscoelastic jet instability behaviour. When the gas to liquid density ratio is small, the wave growth rate of axisymmetric disturbance is higher than that of asymmetric disturbances, indicating the axisymmetric disturbance is more detrimental. When the gas to liquid density ratio increases, both the growth rate and the instability range of disturbances increase drastically, more asymmetric disturbance modes with large values of n become unstable, and the growth rate of each asymmetric disturbance mode approaches that of the axisymmetric disturbance. Therefore, the effects of the asymmetric disturbances become stronger as the gas to liquid density ratio increases.

The surface tension resists the development of instability on viscoelastic liquid jets with both axisymmetric and asymmetric disturbances, i.e., they smooth out the disturbances on the interface between the liquid and the gas, whereas the aerodynamic

effect enhances the instability. These two parameters influence the instability behaviour of viscoelastic liquid jets greatly.

The role of interfacial shear in the onset of instability of a cylindrical viscous liquid jet in a viscous gas surrounded by a coaxial circular pipe is elucidated by use of an energy budget associated with the disturbance. It is shown that the shear force at the liquid-gas interface retards the Rayleigh-mode instability which leads to the break-up of the liquid jet into drops of diameter comparable to the jet diameter, due to capillary force. On the other hand the interfacial shear and pressure work in concert to cause the Taylor-mode instability which leads the jet to break up into droplets of diameter much smaller than the jet diameter. While the interfacial pressure plays a slightly more important role than the interfacial shear in amplifying the longer-wave spectrum in the Taylor mode, the shear stress plays the main role of generating the disturbances of shorter wavelength.

The onset of instability in a viscous liquid jet in the presence of a surrounding viscous gas may manifest itself as convective or absolute instability depending on the flow parameters. There are two different modes of convective instability, the Rayleigh and Taylor modes, these two modes are caused by fundamentally different physical mechanisms. The main cause of the Rayleigh-mode instability is capillary pinching which is resisted by the inertia in the form of pressure fluctuation and the viscous shear stress exerted by the gas at the interface. On the other hand, the gas pressure and shear fluctuations are the main means of supplying energy to the disturbances in the Taylormode instability. The surface tension tends to resist the formation of short waves. The unstable disturbances in an absolutely unstable jet propagate both in the upstream and downstream directions, accompanied by a large liquid pressure fluctuation in the axial direction. This pressure fluctuation is of the same order of magnitude as the surface tension term. Capillary pinching remains a dominant source of absolute instability as well as the Rayleigh mode of convective instability.

In the review paper of Gulawani et al. [24], experimental results that have been published so far, as well as all mathematical models, have been critically analyzed. A

comprehensive discussion has been presented and an attempt has been made to arrive at a coherent theme that clearly describes the present status of the published literature. Furthermore, the recommendations that have been made are expected to be useful for the design engineers, as well as researchers. The knowledge gaps have been identified and suggestions have been made for further research, which, in turn, will improve the reliability in the design of this important class of gas-liquid jet reactors.

The instability at the gas/liquid interface of the jet was studied using Kelvin-Helmholtz instability analysis [5-6, 25-26]. Chawla [26] developed a model for nonreacting systems by assuming the change in perturbation as a function of distance, time, gas velocity, and wavelength of disturbance and obtained conditions for linearization of the governing equations of flow. Based on the same guidelines, Chan et al. [6] developed a model for the reacting system by considering mass transfer at the gas/liquid interface governed by condensation and evaporation processes, which incorporate the phenomena of suction and blowing of the gas/liquid interface. Thus, the evaporation term has been incorporated in the perturbation equation and stability criteria have been obtained. Although studies have been conducted for the instability at the gas/liquid interface, the effect of nozzle diameter and operating conditions must be incorporated when developing the stability criteria.

2.2 Instability Analysis of the Liquid-Gas Interface of Submerged Gas Jets

Submerged bubbling/jetting is employed to enhance heat and mass transfer rates by producing large interfacial areas. The whole gas-stirred injection zone consists of several regions, a gas bubbling or jetting core, a two-phase turbulent zone of gas dispersed in liquid, a liquid recirculating zone, and sloshing waves formed on the surface of the bath when the gas flow rate is high enough. With increased gas injection flow rate, a transition from *bubbling* to *jetting* occurs when the bubbles in the plume coalesce, thus a gas jet is formed. In the initial jetting regime, the gas jet does not disintegrate until it reaches some distance from the nozzle, where the jet breaks up into a column of rising bubbles. The transition between bubbling and jetting can be identified. There is a change in the sound generated by the gas flow. Jetting

corresponds to a high frequency sound while bubbling is characterized by a deep, low frequency sound [27]. Also the bubbling is seen to expand radially from the injector and essentially no expansion is seen in the jetting regime [28-29].

McNallen and King [30] tested the injection of different inert gases into water and liquid metals and concluded criteria for transition to jetting nozzle exit mass flux of about $40 \text{ g/cm}^2 \text{ s}$. This value corresponds to sonic injection in an air-water system at environmental pressure. Ozawa and Mori [28-29] stated that the transition from bubbling to jetting takes place when the nominal Mach number at the injection nozzle exit approaches unity. They used the ratio of the time during which the basal diameter of bubbles or jets is in apparent contact with the orifice diameter to a total observing time. There is an abrupt reduction of time fraction of contact at the transonic region. The phenomenon is similar both for gas injected into water and mercury. Ozawa and Mori did not give a theoretical explanation on the transition from bubbling to jetting. Korita [4] presented a simple structure model and calculated the non-buoyant jet length. He concluded that for injection velocities of $M < 1$, the gas jet disintegrates in the form of bubbles very close to the gas injecting orifice, and a bubble column forms in a metal bath. For $M > 1$, the length of the non-buoyant jet in the bath is appreciable and the jet disintegrates later into bubbles.

The transition from gas bubbling to jetting is very important because high gas injection velocity is necessary to obstruct liquid accretion formation on the tip of the injection nozzle and to prevent the phenomenon of gas back attack, but jetting may reduce the reactant interfacial contact area and gas residence time, thus reducing heat and mass transfer between the phases. However, there is little fundamental explanation presented with regard to these important phenomena. Chen & Richter [7] focused on improving the current theoretical understanding of the transition from bubbling to jetting.

Submerged gas injection into liquids is a widely applied processing technique. At low gas flow rates, a bubble plume forms in the liquid. With increasing gas flow rates, the gas bubbles in the plume coalesce and a gas jet is formed. Transition from bubbling to

jetting occurs in the transonic region. To date, there is no sufficient theoretical explanation for this transition. Chen & Richter [7] developed a basic theory to explain the transition from bubbling to jetting. The instability of a circular compressible gas jet in a liquid was studied. For the axisymmetric mode, it was found that there is a peak growth rate for both the temporal and spatial instabilities when the Mach number approaches unity. The instability quickly reduces to vanishing values at supersonic gas velocities. However, in the supersonic region, it was shown that the helical instability mode may become important. Gas pressure perturbations have a destabilizing effect in the subsonic region but a stabilizing effect in the supersonic region. The problem of absolute instability was studied in order to explain the physical phenomenon of the transition from bubbling to jetting. Absolute instability was found in the subsonic region and a gas jet always breaks up into bubbles in the subsonic region. No absolute instability was found in the supersonic region, and the gas jet may remain stable. This transition from absolute to non-absolute instability occurs in the transonic region which was observed to be the transition from bubbling to jetting.

The phenomenon of the transition from bubbling to jetting in gas injection through a submerged nozzle into a liquid has been studied in view of the instability of a gas jet in a liquid. A simple model of uniform-velocity profile, a semi-infinite, axisymmetric gas jet in an inviscid liquid was established and the dispersion equation was solved numerically. For the axisymmetric mode, both temporal and spatial growth rates of the disturbances increase with increasing gas velocity in the subsonic region. There is a peak of the growth rate where the Mach number approaches unity, and the growth rate quickly reduces to zero after that, which indicates interfacial waves reach the most unstable state in the sonic region and become temporally and spatially stable in the supersonic region. For long waves, the first non-axisymmetric mode becomes dominant in the supersonic region and the gas jet may not become temporally stable in the supersonic region. Absolute instability was found in the subsonic region while there is no absolute instability in the supersonic region. Thus, in the subsonic region, small disturbances will grow immediately in any position without limitation causing the jet to break up and bubbling occurs. In the supersonic region, small disturbances

will finally become evanescent or be convected away downstream so that their amplitudes eventually decrease with time, and the gas jet remains stable. Thus, jetting exists in the supersonic region and the transition from bubbling to jetting occurs in the transonic region.

A number of practical applications involve the break-up of gas jets injected into liquids, such as nuclear reactors, oxygenators in pharmaceutical industries, coal and mineral purification by flotation [31], and formation of liquid shells [32]. Whereas the breakup of liquid jets injected into gases has been studied in detail in the past few studies have focused on the breakup of gas jets. Li and Bhunia [33] studied the temporal instability of plane gas sheets in a viscous liquid medium. The results indicated that sinuous and varicose disturbances were unstable; surface tension reduced the growth rate, whereas the relative velocity between the gas and liquid and the gas density enhanced the growth rate of the disturbances. Also, the wave propagation velocity was much smaller than the gas velocity, implying that the disturbances were almost stationary, rather than traveling-wave type. Radwan [34] considered the instability of a hollow gas jet with effects of surface tension and fluid inertia, neglecting the liquid viscosity; the gas inertia was found to have a destabilizing influence. The objectives of this investigation were to study the three-dimensional instability characteristics of subsonic gas jets injected into a coflowing liquid medium, neglecting the effects of gravity. A linear temporal instability analysis is used to document the wave growth rate as a function of wave number.

Parthasarathy and Chiang [35] conducted a temporal linear stability analysis of an inviscid incompressible gas jet injected into a co-flowing viscous liquid to study the growth of small three-dimensional disturbances that lead to the break-up of the gas jet. The primary flow parameter that governed the growth of the disturbances was the gas Weber number. At small Weber numbers, only the two-dimensional varicose disturbances were unstable; at high Weber numbers, three-dimensional disturbances became unstable with growth rates comparable to the sinuous and varicose disturbances. The phase velocity of the disturbances in the gas jet was small, on the order of the co-flowing liquid velocity.

In summary, a linear stability analysis was conducted to study the growth rates of three-dimensional disturbances on an incompressible inviscid gas jet injected into a liquid co-flow, in the absence of gravitational effects. At small Weber numbers, only the varicose disturbances were unstable. As the Weber number was increased, the sinuous disturbance became unstable and its growth rate approached that of the varicose disturbance. A further increase in the Weber number led to other azimuthal modes ($n = 2, 3$, etc.) becoming unstable, with their growth rates only slightly less than the growth rate of the varicose disturbances. It was also found that the phase velocity of the disturbances was small, on the order of the co-flowing liquid velocity. The results of the analysis presented herein agree with the limited experimental observations that exist in the literature [36], more carefully conducted experimental measurements are needed to understand the break-up mechanisms of gas jets.

2.3 The Effect of Mass Transfer on the Instability of Interface of Gas Jet Submerged in a Liquid

Several investigators have studied both experimentally and analytically the Kelvin-Helmholtz instability of the gas-liquid interface. Chang and Russel [37] analyzed the case where a subsonic and a supersonic gas jet flowed through a plane of liquid. Nachtsheim [38] examined the three-dimensional disturbance of a shear flow in which a thin liquid film was exposed to a supersonic gas stream with wave fronts obliqued to the external stream. Nayfeh and Saric [39] analyzed a compressible gas stream flowing over a liquid under the influence of a body force directed outward from or toward the liquid. Craik [40] examined both experimentally and analytically the instability of thin liquid films exposed to an incompressible air stream. Chawla [5] analyzed the case where a subsonic or a sonic gas jet is flowing through a liquid, under the action of pressure perturbation, liquid viscosity, and surface tension. Chawla [26] also developed a simple model for the rate of entrainment of the liquid in accordance to the knowledge of Kelvin-Helmholtz instability of the interfacial wave. None of them has considered the instability of a gas/liquid interface with mass transfer and is applicable to the present submerged reacting jet, such as the reacting

hydrochloride-aqueous ammonia system in which a periodic or cyclic plume behavior was found. The present analysis explores the theoretical background in understanding the Kelvin-Helmholtz instability of a liquid-vapor interface with mass transfer (blowing velocity) across the interface. Solution of Kelvin-Helmholtz instability analysis is then used, as an application, to determine the break-off distance of submerged reacting jets and the results of the prediction are compared to the reported data of HCl(g) NH₃(aq) jets [41].

Chan, Wang and Tan [6] employed the theory of Kelvin-Helmholtz to analyze the instability phenomena of non-reacting and reacting stratified gas flows injected sonically into a liquid. The effect of the mass transfer at the gas-liquid interface on the instability is investigated. It is shown that the mass transfer affects the pressure perturbation which acts to transfer energy from the gas phase to the liquid layer through its evaporating and condensing behavior, its wave-drag and lift components, against forces due to surface tension and liquid viscosity. The dimensionless wave frequency, amplification, and wavelength at the maximum instability are presented as a function of a dimensionless surface tension/viscous parameter and a blowing parameter due to the interfacial mass transfer. The interfacial evaporation is found to enhance the instability while the interfacial condensation is to reduce the instability. The results provide the theoretical explanation of the reported dynamic and instability behavior found in the reacting jet of a HCl gas submerged in the ammonia aqueous solution. Finally, an application to the prediction of the break-off plume length observed in submerged reacting jets is presented and the results are compared to experimental data of the HCl(g)- NH₃(aq) system.

The effect of mass transfer on the Kelvin-Helmholtz instability of the gas-liquid interface of a sonic gas jet submerged in a liquid has been analyzed. Solutions have been presented for the dimensionless amplification factor, angular frequency and wavelength corresponding to the maximum instability of the interfacial wave. The results show that the interfacial evaporation or exothermic reaction enhances the wave instability while the condensation or endothermic reaction reduces the instability. The results also elucidate the periodic break-off phenomena observed in reacting

submerged jets. Finally, application to the prediction of the break-off length has been made and theoretical predictions are found in satisfactory agreement to experimental data.

2.4 Experimental Analysis of Liquid-Gas Interface at Low Weber Number

Liquid sprays produced from the ejection of liquid into a gaseous environment are constituted of drops with different sizes. In all applications, the spray drop size distribution is an important parameter that needs to be controlled. However, the prediction of drop size distribution in any situation is not possible so far because very little is known about the way ligaments and drops are torn off from a perturbed liquid flow. This lack of information is due to the deficit of experimental investigations on this topic and predictions depend largely on empirical knowledge.

The description of a liquid-gas interface during atomization can be easily investigated by experiments when a single length scale dominates the perturbation process. This is the case for instance of low velocity plain cylindrical liquid jets subject to a capillary instability (Rayleigh instability). The development of this instability is characterized by the growth of an axisymmetric sinusoidal perturbation up to the production of drops when its amplitude is of the same order of magnitude as the jet radius. This process of interface deformation has been widely experimentally investigated [42-43]. However, when the difference of velocity between the liquid and the surrounding gas is high, deformation and disintegration of the liquid flow are more complex. The widely investigated case of a round liquid jet surrounded by an annular high-speed gas flow corresponds to this situation. Numerous visualizations of air-assisted liquid jets can be found in the literature. They all show that the liquid deformation depends on a wide range of time and length scales. Thus, the study of the spatial and temporal behavior of the liquid-gas interface prior to and during the break-up becomes difficult and experimental characterizations are often limited to the determination of average quantities such as break-up length, spray angle, and temporal oscillation frequency. These quantities are not sufficient to characterize the atomization process and thus to predict the drop size distribution. The drops torn off from a liquid flow during an

atomization process are functions of the shape of the liquid-gas interface and investigations dealing with the experimental characterization of the liquid-gas interface during atomization are required.

Furthermore, an atomization process can be seen as a process where the interface surface area between a given amount of liquid and the surrounding gas increases until a physical phenomenon opposes this increase and results in the break-up of the flow. As the aerodynamic effects are negligible in the present case, surface tension forces likely control the liquid break-up. Thus, it is expected that the drop size distribution depends not only on the tortuosity of the interface provided by the fractal dimension, but is also a function of the total liquid-gas interface surface area at the instant of break-up. The area of the interface surface is difficult to measure as the disintegration is 3D but it seems reasonable to think that this area is related to the local interface length measured on 2D images. Within the scope of this work, the local interface length of the bulk flow during atomization is measured. Analysis of the measurements considers the relevance of the fractal dimension and of the local interface length to characterize the liquid flow during the atomization process and investigates the possible relationship between these parameters and the drop size distribution of the resulting sprays measured with a diffraction technique.

Christophe Dumouchel, Jean Cousin and Kaelig Triballier [44] reported an experimental investigation on atomizing liquid flows produced by simplified cavity nozzles. The Weber number being kept low, the sprays produced by these injectors depend on the liquid flow characteristics only, and more precisely, on the non-axial kinetic energy and of the turbulent kinetic energy at the nozzle exit. The investigation reported here concentrates on the characterization of liquid flows during atomization by measuring the spatial variation of the local interface length and of the local interface fractal dimension. Both parameters were found representative of the physics of atomization process: they depend on the characteristics of the flow issuing from the nozzle and they are related to the subsequent drop size distribution. The local interface length is representative of the amount of liquid-gas interface surface area, and is a function of both the non-axial and the turbulent kinetic energies at the nozzle

exit. The fractal dimension is representative of the tortuosity of the liquid-gas interface and, as expected, is mainly related to the turbulent kinetic energy at the nozzle exit. As far as the drop size distribution is concerned, it is found that the local interface length at the instant of break-up determines a representative drop diameter of some kind, whereas the fractal dimension at the same instant controls the dispersion of the distribution.

2.5 Experimental Study on Hydrodynamic Behaviours of High-Speed Gas Jets in Still Water

Investigation on the hydrodynamic behaviours of sub-merged gas jets and their effects concerns quite a wide range of natural and engineering processes such as volcano eruption in deep seas, ice prevention in lakes, water destratification in reservoirs, aeration wastewater treatment, underwater cutting, pneumatic steel aking and so on [45–47]. In addition, noise generation by underwater gas jets is also of interest for some applications [48]. A better understanding of relevant phenomena and mechanisms in the submerged gas exhaust systems is imperative for optimizing various industrial processes. As an example, so-called injection metallurgy emerged in 1980s due to its greater metallurgical and economic advantages. Since then gas stirring by the injection of an inert or reactive gas (or even carried with special particles) into melts is widely used in converters and ladles, where top-, bottom-, sidewall-blowing or their combination is employed for strong mixing and large reaction rates. During the development of studies regarding metallurgical operations, the severe wear of refractory near the tuyere tip through which a submerged gas jet is injected has become one of the main research topics [49-50]. Concerning the problem of refractory erosion, various water-model experiments were carried out and the phenomenon of pressure oscillations, described with the term of back-attack, was observed in the liquid as well as inside the tuyere [51-52]. However, in the previous water-model experiments the investigators used simple cylindrical or convergent conical nozzles from which the gas discharges at a sound speed. Under these operation conditions, the flow regime of submerged jets is bubbling or transition to jetting although nominal Mach numbers at the tuyere exit (NMa) may be greater than

unity by increasing the gas stagnation pressure above its critical value. These authors concluded that, after the transition from the bubbling to jetting regime, the backattack pressure takes a minor change as the nominal Mach number increases up to $NMa \approx 3$ [50-53]. The present work attempts to study the hydrodynamic behaviours of underwater high-speed gas jets issuing from horizontally mounted nozzles operating in correct- and imperfect-expansion conditions. In the recent years, Qi et al. [54] and Shi et al. [55] performed experimental measurements respectively for the average and fluctuating pressures inside underwater high-speed gas jets. Dai et al. [56] focused on the upstream pressure oscillations induced by supersonic and sonic gas jets in quiescent water, especially on those shock- associated phenomena and effects. This research will be benefit to the applications of underwater jet-propulsion vehicles. In general, submerged gas injection results in a complex two-phase flow pattern which can be distinguished into two different regimes: bubbling and jetting. The jetting regime is dominant in the flow system when the gas discharges at a high speed (for instance, up to sound speed or higher). For a supersonic or sonic gas jet in still water, as shown schematically in Fig. 2.1, a gas core is surrounded by a gas-water mixing layer which consists of a drop layer and a bubble layer. When these high-speed gas jets discharge from an imperfectly expanded nozzle, a shock-cell system then appears in the flow field where the detailed structure depends on the Mach number and the pressure ratio at the nozzle exit. Ozawa and Mori once obtained the shock pattern by still photographs with illumination of microflash [57]. The hydrodynamic behaviours of the submerged gas jets and their effects on upstream body attract many researchers and series of experimental investigations are needed in order to understand relevant phenomena and mechanisms.

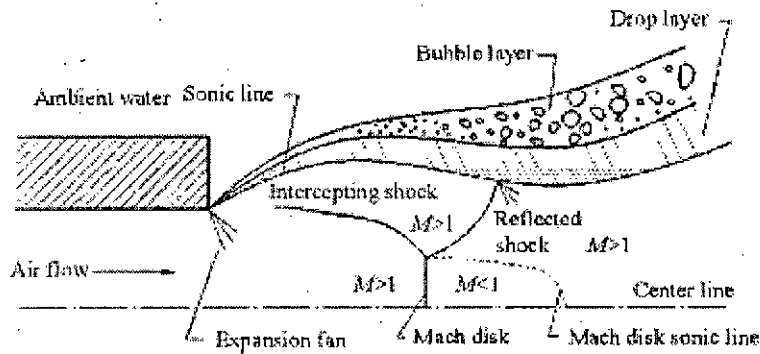


Figure 2.1: Sketch of underwater high-speed gas jet at strongly imperfect-expansion condition

Zhenqing Dai et al. [56] has made experimental investigation on the flow pattern and hydrodynamic effect of underwater gas jets from supersonic and sonic nozzles operated in correct- and imperfect expansion conditions. The flow visualizations show that jetting is the flow regime for the submerged gas injection at a high speed in the parameter range under consideration. The obtained results indicate that high-speed gas jets in still water induce large pressure pulsations upstream of the nozzle exit and the presence of shock-cell structure in the over- and under-expanded jets leads to an increase in the intensity of the jet-induced hydrodynamic pressure.

Experimental investigation is performed on the behaviours of underwater gas jets issuing from supersonic and sonic nozzles operated in the full-, over- and under-expansion conditions. The flow visualization shows that the jetting is the flow regime for the high-speed gas jets operated in the parameter range under consideration. The pressure measurements reveal a distinctive feature of the submerged high-speed gas jets: large discrete pulsations superpose small continuous fluctuations for the upstream sidewall pressures. In addition, the obtained results indicate that the intensity of the hydrodynamic pressure increases due to the presence of the shock-cell structure in the over- or under-expanded jets. Of course, further study is needed on the quantitative analysis of the shock-associate phenomena in the underwater supersonic gas jets.

Chapter 3

Theoretical Development

Consider a cylindrical gas jet issuing from a circular orifice or nozzle into a stationary incompressible liquid. The stability of the jet surface to perturbations is examined using a first order linear theory which ultimately leads to a dispersion equation. The dispersion equation relates the growth rate of an initial perturbation of infinitesimal amplitude to its wavelength, λ . The relationship also includes the physical and dynamical parameters of gas jet and the surrounding liquid.

The following assumptions are mainly involved in derivation of dispersion equation for two-fluid system:

1. The column of liquid is assumed to be infinite in the axial direction .
2. A cylindrical polar coordinate system is used which moves with jet velocity, U
3. The flow is parallel and the velocity is constant throughout the jet
4. The flow was assumed to be inviscid and the effect of the surrounding was neglected.
5. Superficial forces were assumed to act on the surface of the jet
6. The analysis was performed by making an assumption of infinitesimal perturbation acting on the surface of the jet.

A few more assumptions have also been adopted in derivation of governing equation for dispersion of submerged gas jets:

1. A simplified model has been assumed where an isentropic, compressible gas jet injected from a circular cylindrical nozzle
2. The liquid environment is assumed to be unbound inviscid
3. The gas jet is considered to be homogeneous, of uniform velocity profile, semi-infinite system

4. Effect of gravity is negligible if the gas velocity is high and the gas inertia is dominant

Consider an isentropic, compressible gas jet with viscosity μ_G , density ρ_G , injected from a circular cylindrical nozzle with radius “a” and is moving with uniform steady velocity, U. Surrounding the jet is a static liquid of viscosity μ_L , density ρ_L , surface tension, σ . At time $t = 0$, a small amplitude disturbance η_0 is initiated on the surface. This disturbance grows according to

$$\eta = \eta_0 e^{i\kappa z + \alpha t} \dots\dots\dots (3.1)$$

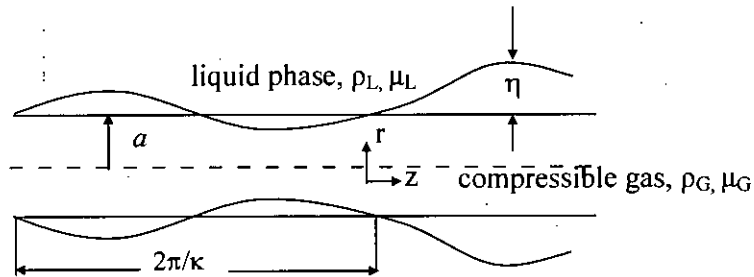


Figure 3.1: Asymmetric wave growth at the surface of a submerged gas jet

Here κ is the wave number, and α is the growth rate and vector sum of time amplification factor, α_r and the angular frequency, α_i of the disturbance. The instability of gas jets occur when the amplification, α_r , is greater than zero. If the initial disturbance η_0 of the wave grows exponentially to a magnitude “a” in time T, it follows that the breakup length of the jet on an average will be

$$L_j = UT = U \left(\frac{\ln(a/\eta_0)}{\alpha} \right) \dots\dots\dots (3.2)$$

Here “a” is the radius of the nozzle. The value of η_0 depends on nozzle smoothness, nozzle diameter etc and is generally determined experimentally.

The growth rate α can be estimated by solving the dispersion equation derived from the equations of motion for both liquid and gas phases and equation (4.1) as the boundary condition.

Following is the example of such equation developed by Chen & Ritcher for submerged gas jet.

$$\frac{\Omega^2 K_n(\kappa)}{\kappa K_n'(\kappa)} - \frac{Q(\kappa - \Omega)^2}{\lambda I_n'(\lambda)} I_n(\lambda) - We_c(1 - \kappa^2 - n^2) = 0 \dots\dots\dots (3.3)$$

Here n specifies the periodicity of the motion around the cylindrical circumference and the dimensionless numbers are defined as

$$\text{Weber number, } We = \frac{\rho_L U^2 (2a)}{\sigma} \dots\dots\dots (3.3a)$$

$$Q = \frac{\rho_G}{\rho_L} \dots\dots\dots (3.3b)$$

$K_n()$, $I_n()$ are modified Bessel functions and λ is defined as

$$\lambda = \sqrt{\kappa^2 - M^2(\kappa - \Omega)^2} \dots\dots\dots (3.3c)$$

In equation 3.3 the prime denotes the differentiation $\frac{\partial}{\partial(\lambda R)}$. For a given set of flow parameters We , Q and M , this governing dispersion equation gives the relationship of the dimensionless wave frequency Ω and the dimensionless wave number, κ .

Chapter 4

Experimental

4.1 Experimental Set-up

A schematic diagram of the experimental set-up is given in Figure 4.1. The set-up comprises a liquid chamber, a nozzle, a compressor, a scale, rotameter and a high-speed video system. The liquid chamber was made up of a Perspex column having dimensions 14cm×7cm×30cm.

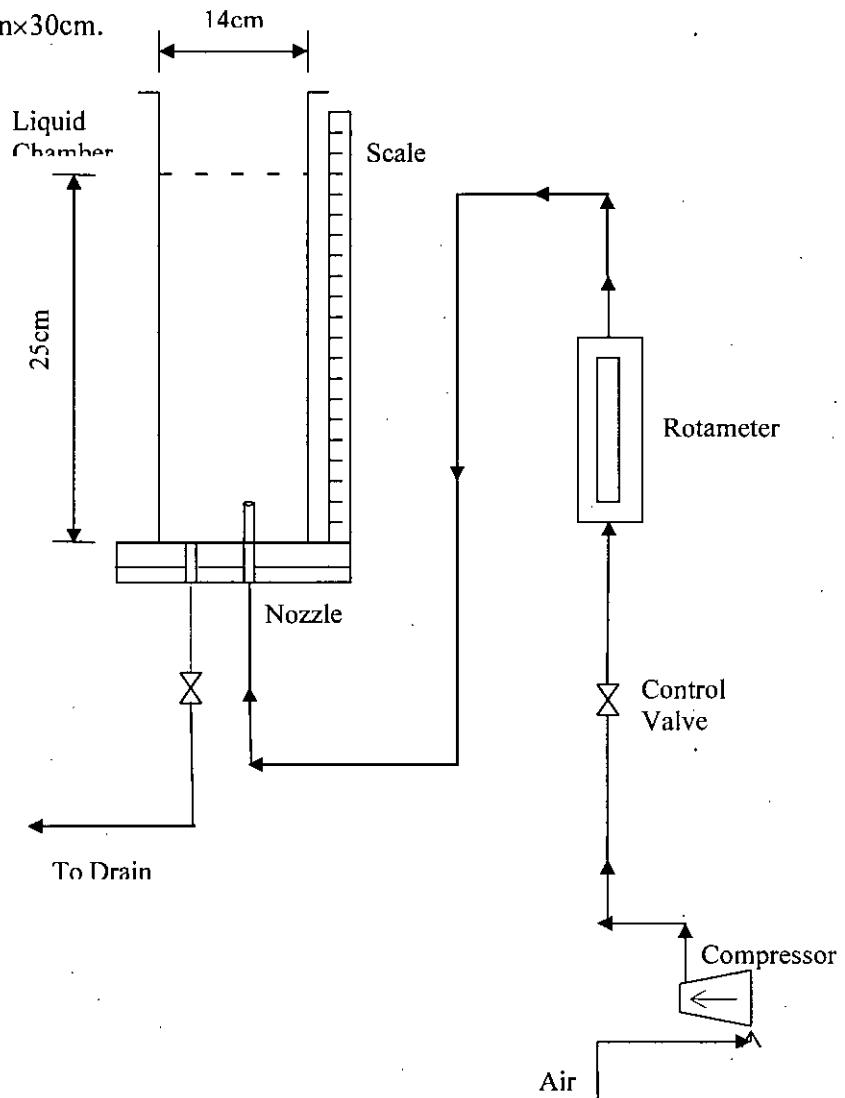


Figure 4.1: Schematic Diagram of Experimental Set-up

The column was filled with liquid to a height of 25 cm. The bubbles and jets were generated by airflow through the nozzle immersed in the stagnant liquid at the bottom of the chamber. The diameters of the nozzles used were 1, 4 and 6 mm. The experiments were executed with three different fluids with different density, viscosity and surface tension namely water, ethanol and glycerol. The air was supplied to liquid chamber by a compressor through a rotameter. The temperature of the water during the experiments was $30 \pm 2^\circ\text{C}$. A digital video system (Sony, Model DMV-60) was used to record the jet images. With this system it is possible to record approximately 60 frames/sec. The video images were then processed by Sigma Scan Pro.

Figure 4.2 shows sample jet images of air/water system for 4 mm at different flow rates. Similar jet images were obtained for ethanol and glycerol system for other nozzle size as well.

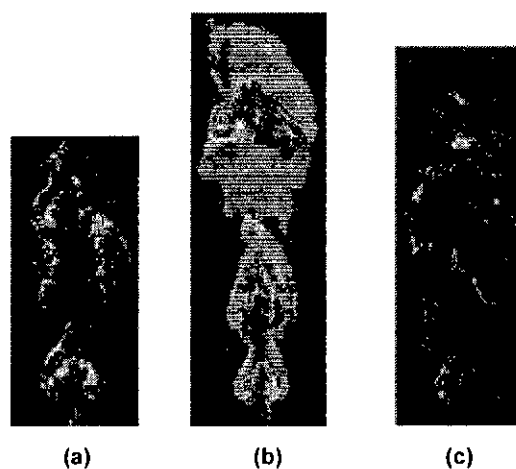


Figure 4.2: Jet images of air/water system for 4mm nozzle at different flow rates

For 1mm nozzle excessive bubble swarming result at high jet velocity. Beyond air jet velocity, $U = 5308 \text{ cm/s}$ it became practically impossible to detect the actual length of the jet. Hence for 1mm nozzle size maximum jet break-up length was not measured beyond 5308 cm/s . Besides, for air/glycerol system, due to excessive foaming jet lengths at higher velocity were not measured.

4.2 Flow Rate Measurement

4.2.1 Calibration of Rotameter

The rotameter used in the experiment was calibrated with the aid of a standardized wet test meter (Figure 4.3). The apparatus was assembled as shown in Figure 4.4 and to calibrate the rotameter ranging from 10L/hr to 360L/hr; it was adjusted to a low setting representing about 25% of its full scale.

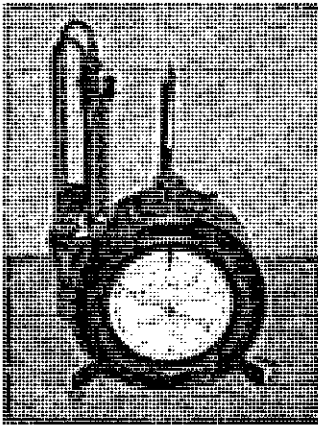


Figure 4.3: Wet Test Meter

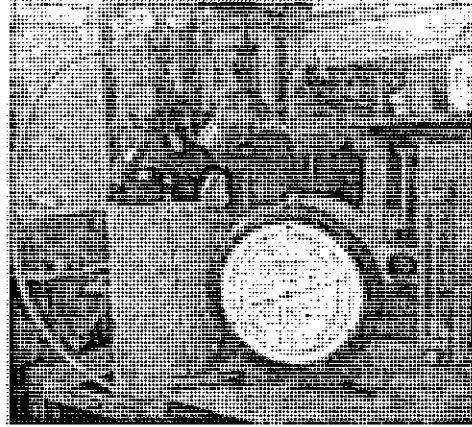


Figure 4.4: Experimental set-up for calibration of rotameter

A stop watch was used to measure the time required to draw the appropriate volume of air through the meter. The ambient temperature and pressure was recorded. Standardized flow meter reading from wet test meter was measured. At least four observations have been made and finally average flow meter reading has been taken. The above steps repeated for rotameter settings of 50%, 75% and 100% full scale.

The recorded ambient temperature during experiment was $30 \pm 2^\circ\text{C}$ and pressure was 1atm. A calibration curve has been generated by plotting observed flow rate against actual flow rate as shown in Figure 4.5.

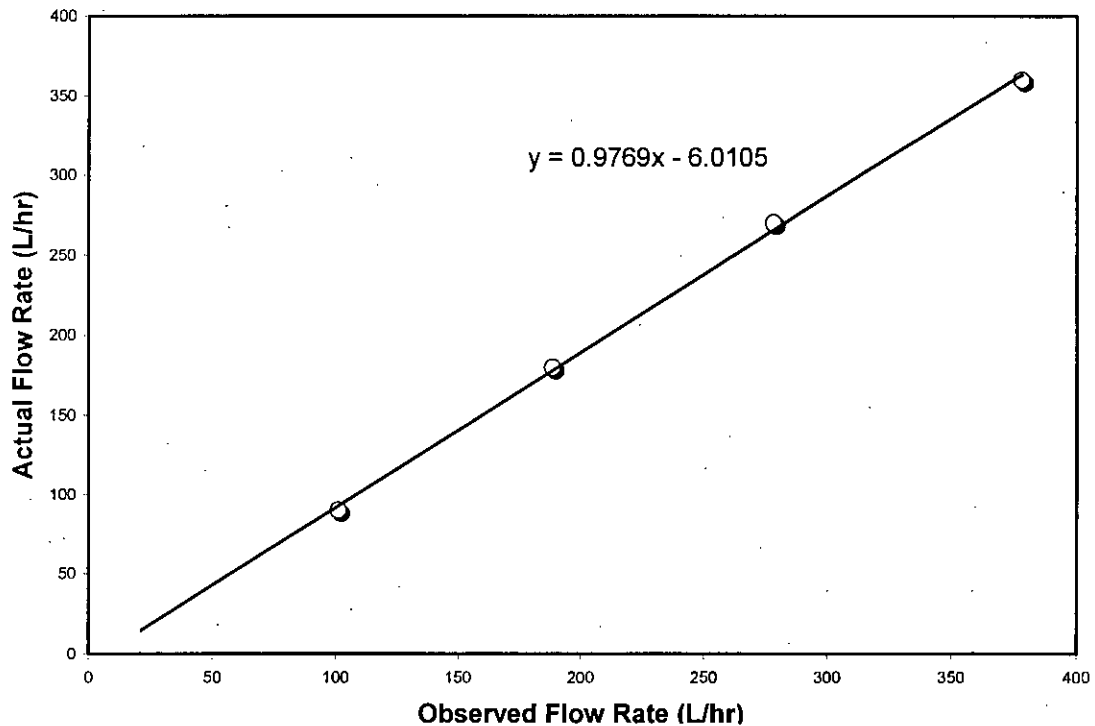


Figure 4.5: Calibration Curve for Rotameter

4.2.2 Percentage of Error due to Fluctuation in Rotameter Float

The float of the rotameter was fluctuated due to the variation in flow pressure during experiment. An approximately $\pm 5\%$ error has been recorded for the fluctuation in rotameter float.

4.3 Length Measurement

The jet length in the experiment was measured by image processing. In digital editing, photographs are usually taken with a digital camera and input directly into a computer. Image Processing requires that images to be analyzed must be in a specific graphic format called TIFF (digital images).

For image processing video clipping has been taken for three minutes. From three minutes video clipping best five frames have been selected which clearly shows the

jet and scale in the experimental set up. Then SELECT LINE tool has been clicked on and a line has been drawn from one side of the image to the other. Length of the jet has been measured and listed for a frame as shown in Figure 5.6.

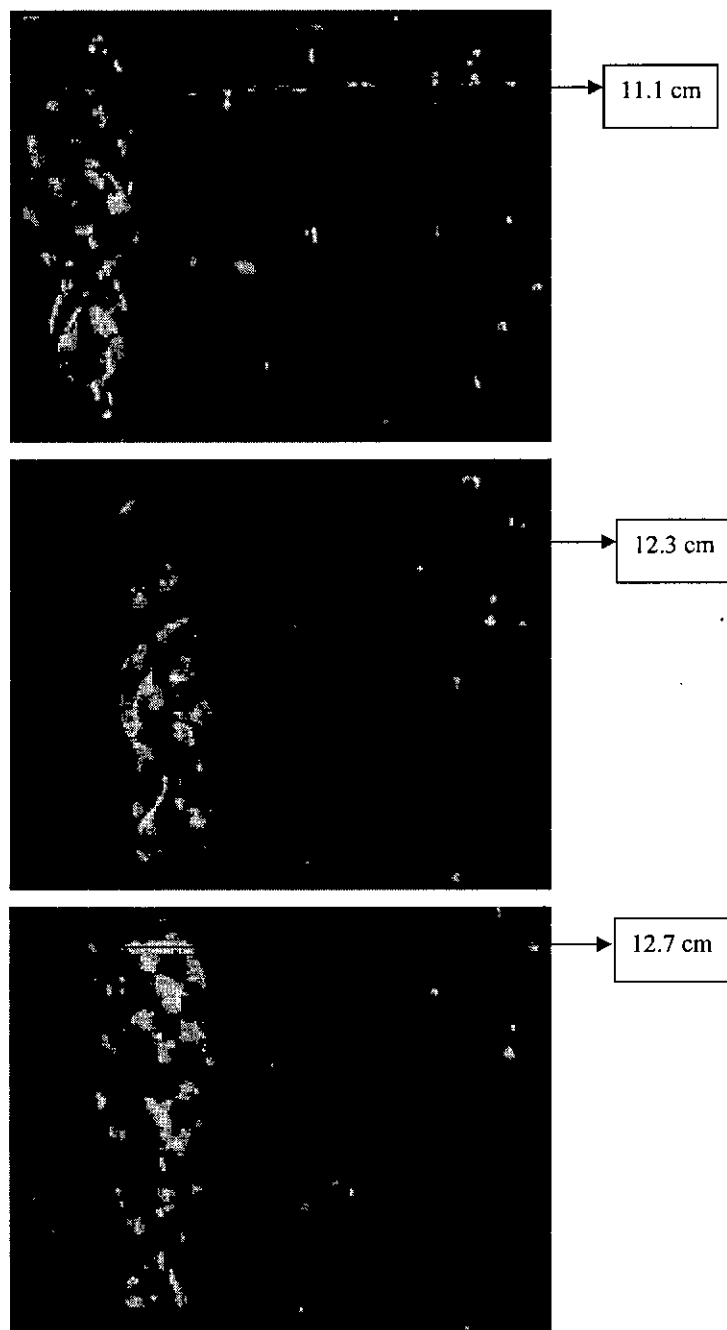


Figure 4.6: Measurement of jet length by image processing in air/ethanol system

Average length of the jet has been taken. Corresponding flow rate has been recorded. The MAGNIFYING GLASS tool in the window is used to get a closer look at a specific part of an image and to enlarge the individual pixels. An approximately 6-7% error has been observed in measurement of jet length.

Chapter 5

Results and Discussion

The present study dealt with experimental study of submerged air jets and interpreting the jet behavior with the aid of existing theoretical understanding of stability of submerged jets. The objectives of this project are to measure jet length submerged in liquids under different flow condition at various nozzle sizes and to understand the effect of interfacial disturbance in jet-breakup process by comparing the experimental findings with the numerical analysis reported in the literature.

The bubbles and jets were generated by airflow through the nozzle immersed in the stagnant liquid at the bottom of the chamber. The diameters of the nozzles used were 1, 4 and 6 mm. The experiments were executed with three different air/liquid systems such as air/ethanol, air/water and air/glycerol. The jet length in the experiment was measured through image processing at different flow rate.

The maximum length of the jet varied with the nozzle size. Nozzle size has also significant contribution on jet formation velocity as well as nature of surface disturbance. For 1mm nozzle vigorous bubble swarming result at high jet velocity. Beyond air jet velocity, $U = 5308$ cm/s it became practically impossible to detect the actual length of the jet. Hence for 1mm nozzle size maximum jet break-up length was not measured beyond 5308 cm/s. Besides, for air/glycerol system, due to excessive foaming jet lengths at higher velocity were not measured. Liquid properties have effect on span of jet break-up curve.

Jet velocity is also has significant contribution in jet break-up process. At low velocity regime growth rate of disturbance is considered to be independent of jet velocity by making analogy with liquid/liquid system. But at higher velocity the growth rate of disturbance becomes function of velocity.

The measured jet lengths in three different liquids are plotted against jet velocities for 1, 4 & 6 mm tube in figure 5.1, 5.2 and 5.3, respectively.

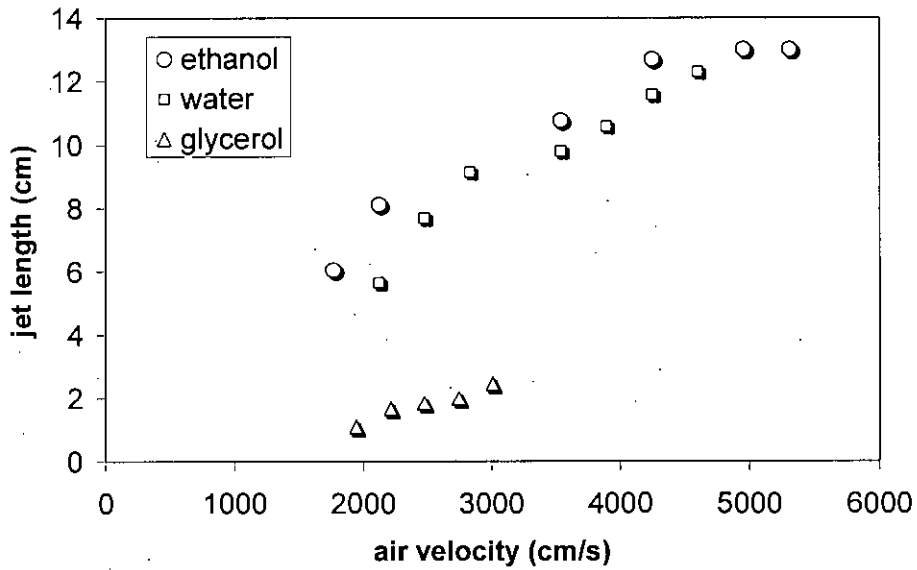


Figure 5.1: Plot of jet length versus air velocity for 1mm nozzle

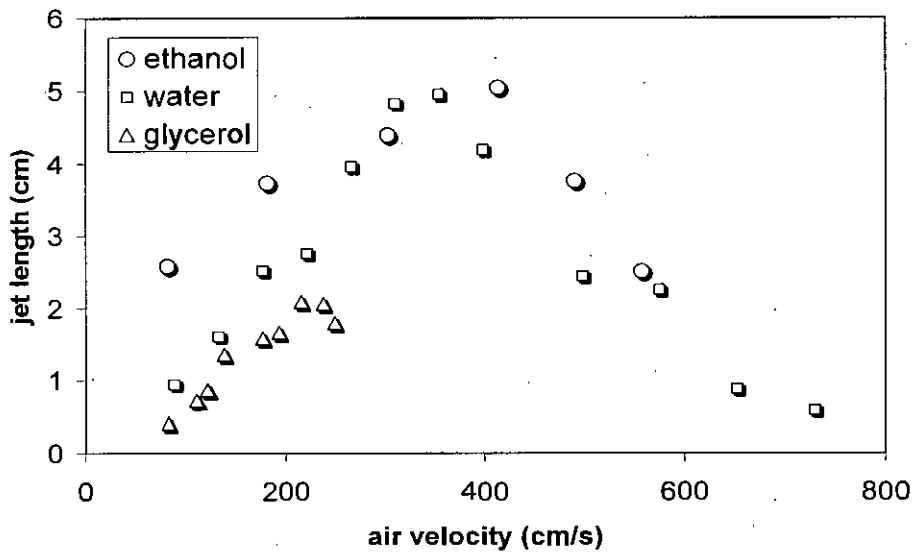


Figure 5.2: Plot of jet length versus air velocity for 4mm nozzle

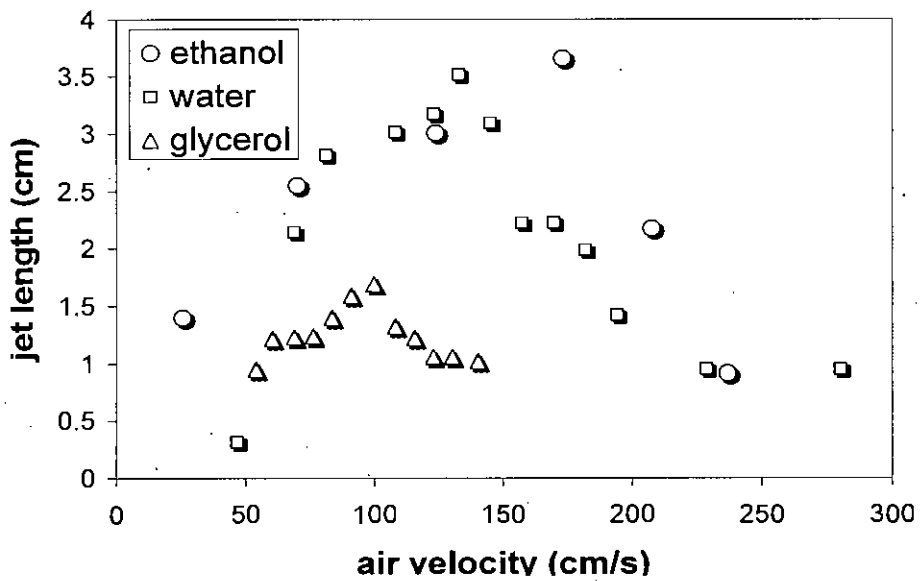


Figure 5.3: Plot of jet length versus air velocity for 6mm nozzle

The Figures show that the jet lengths increase with the increase of jet velocity till they go through a maximum value. Jet formation velocity, jet length and the velocity at which jet length reaches its maxima depend on nozzle diameter as well as physical properties of the gas/liquid system. Table 5.1 summarizes the variation of jet formation velocity & jet breakup length with nozzle diameter and physical properties of liquid.

Table 5.1: Variation of Dynamic Properties of Gas Jets

Dynamic Properties	Variables	Ethanol	Water	Glycerol
		nozzle σ/μ_L	1841	7290
Jet Formation Velocity U, (cm/s)	1	1769	2123	1946
	4	81.4	88.5	82.9
	6	25.6	46.7	54
Maximum Jet Length L_{max} , (cm)	1	13	12.3	2.45
	4	5.05	5.09	2.1
	6	3.66	3.52	1.7
Velocity at which L_{max} occurs, U_{Lmax} (cm/s)	1	5308	4600	3008
	4	413	353.9	215.6
	6	173	132.7	99.8

5.1 Effect of Nozzle Size

Table 5.1 shows that jet formation occurs at higher velocity for smaller nozzle size. For 1 mm nozzle jet forms at much higher velocity than for the rest two. Formation of jet i.e. transition from bubbling to jetting is a much studied phenomenon and a number of semiempirical correlations are available in literature. Following are two such major equations [58-59].

$$\frac{H}{D} = C_1(Ku) + C_2 \dots \dots \dots (5.1)$$

Here $Ku = \frac{U\rho_G^{0.6}}{(\sigma g(\rho_L - \rho_G))^{0.26}} \dots \dots \dots (5.1a)$

$$\frac{H}{D} = C \left(\frac{\rho_G}{\rho_L} \right)^{0.6} U \dots \dots \dots (5.2)$$



Both the equations show that bubble to jet transition velocity, U is inversely proportional to the nozzle diameter, D . Thus the observations shown in Table 6.1 can be explained qualitatively. Quantitative analysis would, however, require consideration of other geometric factors such as liquid height H , smoothness of nozzle etc.

In the present study, depending on the nozzle size observed jet lengths were varied. For 1mm nozzle size more stable and higher jet length is achieved. As the nozzle diameter is increased, the maximum height of the jet in a particular gas/liquid system (air/ethanol, air/water or air/glycerol) is reduced as observed by Grant and Middleman [3] for liquid/liquid system. Furthermore, nozzle size was found to affect the nature of surface disturbance that leads to jet break-up. Figure 5.4 (a) and (b) show sample images of jets for 1mm, 4mm and 6mm nozzles in water.

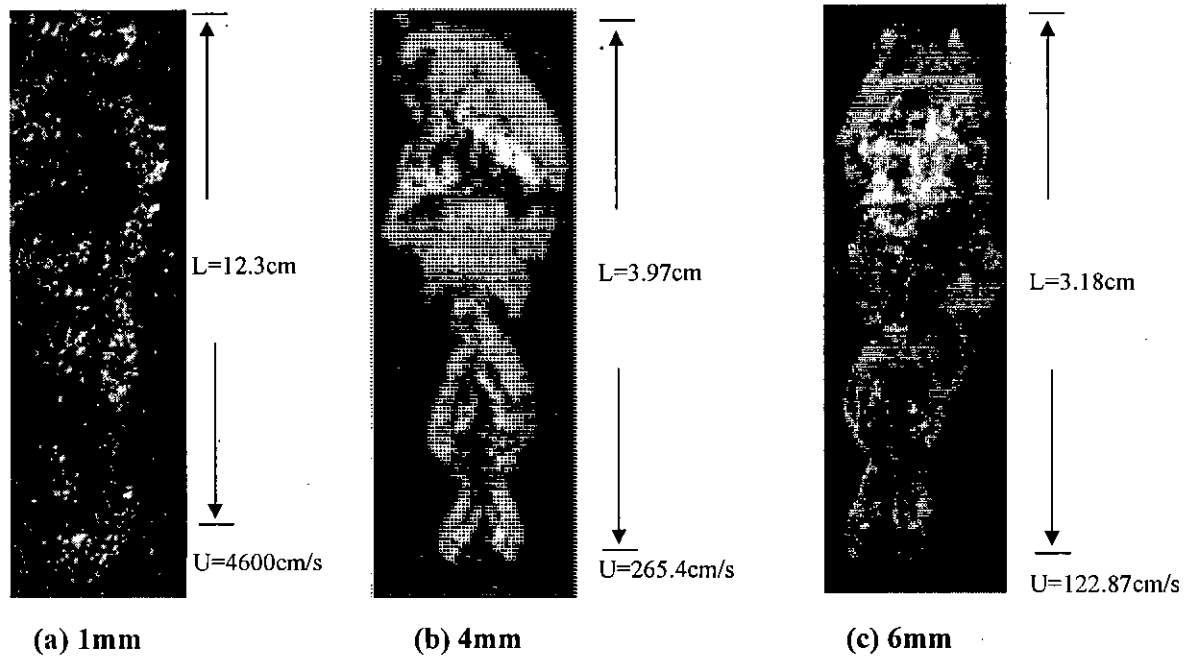


Figure 5.4: Sample images of jets in different nozzle size

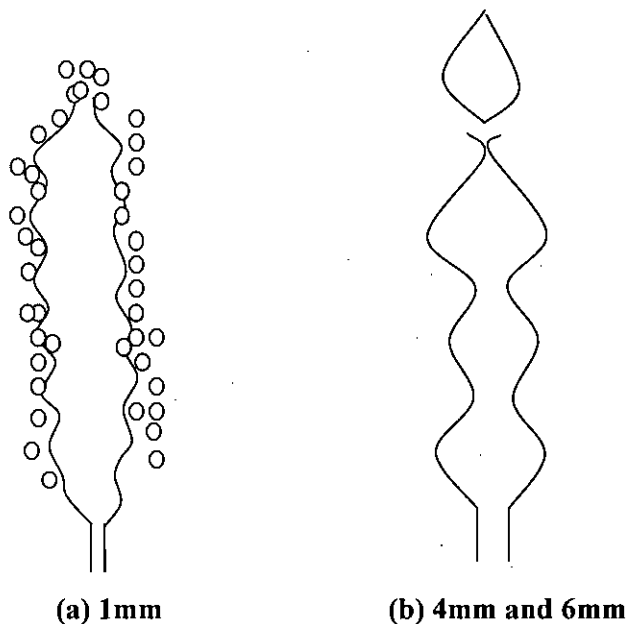


Figure 5.5: Illustrated view of jet formation in different nozzle size

For 4 and 6mm nozzles steady and clear jets were observed from formation to disintegration velocity. However, vigorous bubble swarming results at 1mm nozzle for each of the fluids of interest at high velocity. Surface breaks down into bubbles before the break-up of the core. As illustrated in Figure 5.5 (a) and (b), surface disturbance disrupts the surface of the jet resulting in bubble formation along the jet length for 1mm nozzle. On the other hand, for 4 & 6mm nozzle, surface disturbance causes complete break-up of the jet and forms bubble at the end of jet length.

5.2 Effect of Liquid Properties

The instability analysis of gas-liquid interface made by Chan et al. [6] shows that the surface tension to viscosity ratio, σ/μ_L , of liquid has major effect on jet break-up length. It was explained that since surface tension force restores the jet length and viscosity tries to break it down, larger the ratio of σ/μ_L , higher the jet length. Table 5.1 shows that the ratio, σ/μ_L ethanol and water are of same order of magnitude and generates jet length of same order. On the other hand, the jet length in glycerol is

much lower than those in ethanol and water since glycerol has a much higher viscosity. The smaller span of break up curves for glycerol is also due to its large viscosity.

5.3 Effect of Jet Velocity

Figure 5.1, 5.2 & 5.3 show the behavior of jets in the form of a break-up curve. Once a jet is formed jet length increases steadily with increasing jet velocity and after it reaches maxima jet length decreases with jet velocity. According to Rayleigh [1] analysis for liquid jet at low velocity regime the inertia of the outer atmosphere will not affect the jet stability and surface tension forces of the liquid jet are the only ones responsible for instability. Hence for lower velocities the break-up length L depends linearly on the jet velocity U . At larger jet velocity, the inertial effect of the surrounding liquid becomes important and non linear dependence of jet length on velocity is observed.

In an attempt to single out the effect of jet velocity on jet length nine sets of data obtained in present study are combined in a single graph by plotting L/L_{max} vs. U/U_{Lmax} .

Here L_{max} is the maximum length obtained for a particular liquid and particular nozzle size and U_{Lmax} is the corresponding jet velocity.

Equation (3.2) can be written as

$$L = C_0 \frac{U}{\alpha} \dots\dots\dots (5.3)$$

Where $C_0 = \ln(a/\eta_0)$ is considered to be constant for particular nozzle sized and gas/liquid system.

Following equation can be written for maximum jet length L_{\max} :

$$L_{\max} = C_0 \frac{U_{L_{\max}}}{\alpha_{L_{\max}}} \dots\dots\dots (5.4)$$

Here $\alpha_{L_{\max}}$ is the growth rate of disturbance at L_{\max} .

From above equation (5.3) and (5.4)

$$\frac{L}{L_{\max}} = \frac{U}{U_{L_{\max}}} \frac{1}{\alpha_{\max}} \dots\dots\dots (5.5)$$

By making analogy with liquid/liquid system in L/L_{\max} vs $U/U_{L_{\max}}$ plot, for $U/U_{L_{\max}} < 1$, data are best fitted as a straight line.

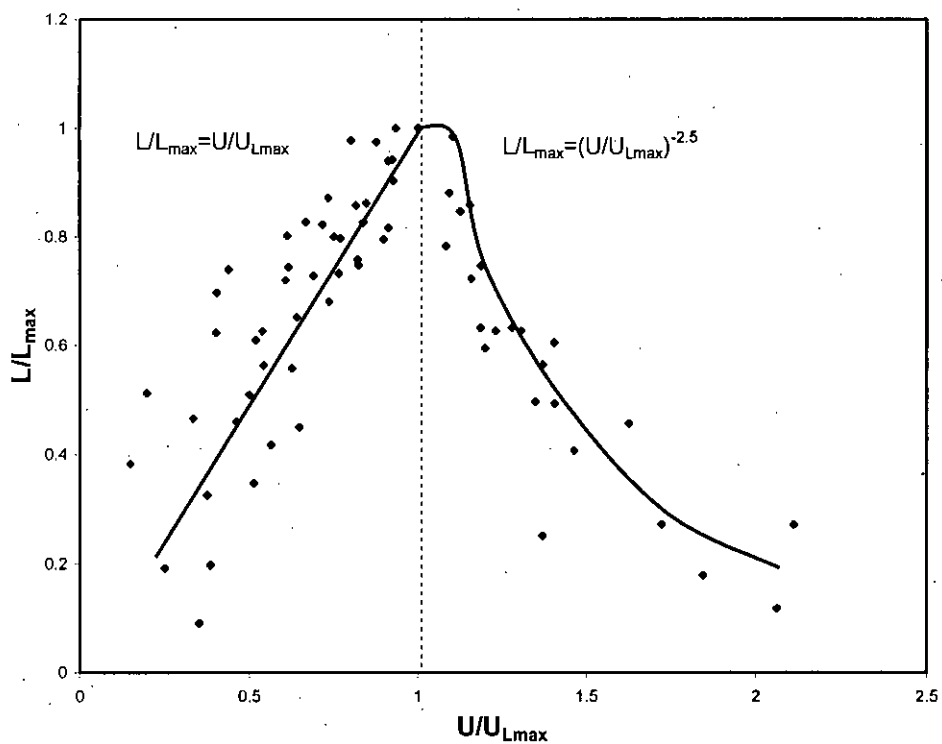


Figure 5.6: Variation of L/L_{\max} with $U/U_{L\max}$ for ethanol, water and glycerol

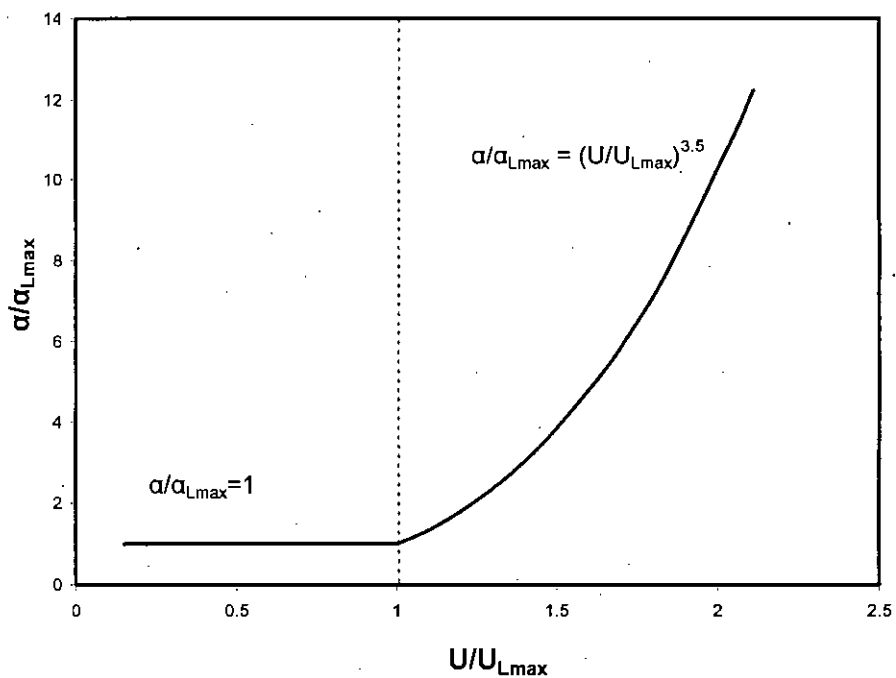
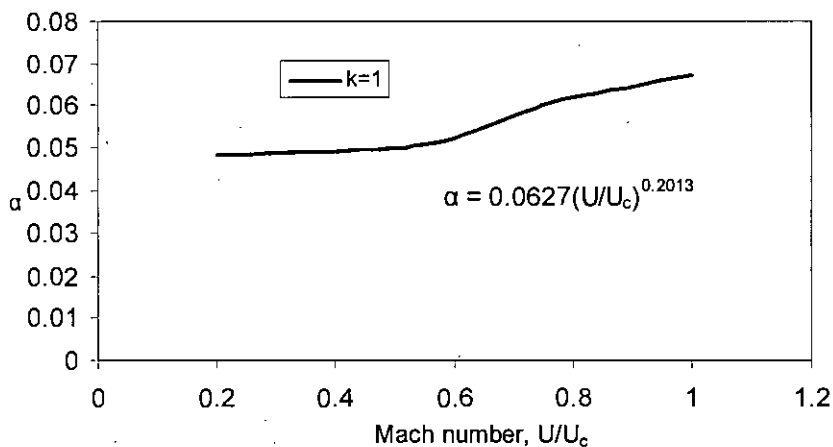
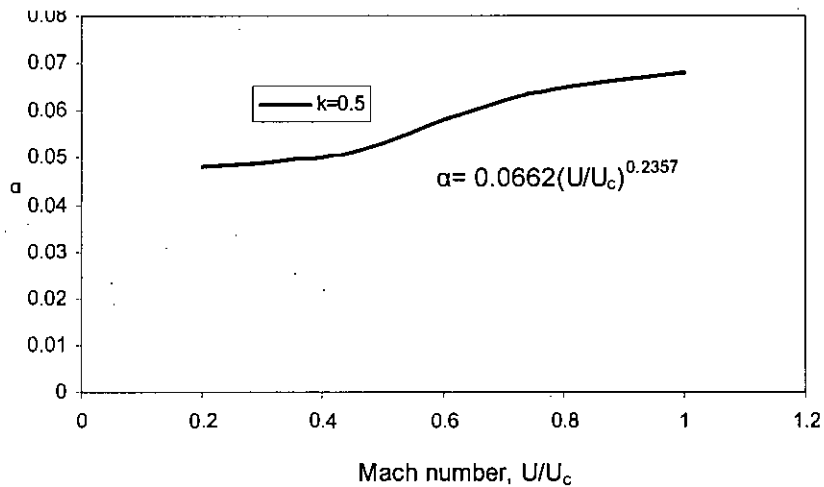
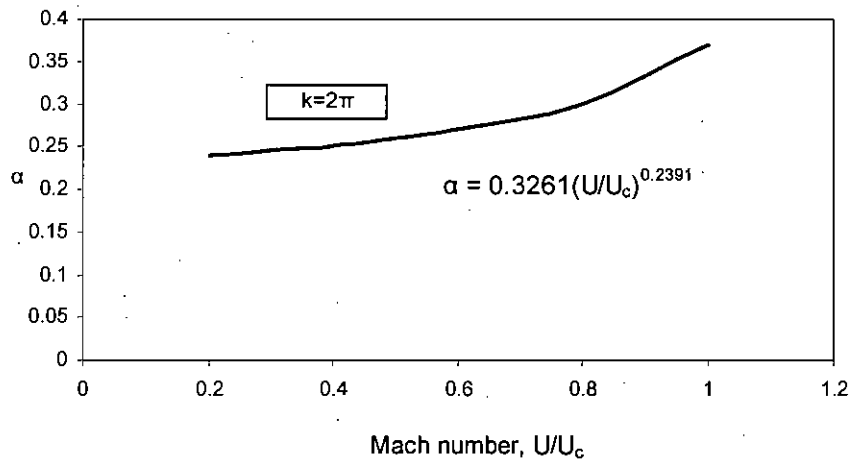


Figure 5.7: Variation of $\alpha/\alpha_{L\max}$ with $U/U_{L\max}$ for ethanol, water and glycerol

Figure 5.6 shows that the plot of L/L_{\max} vs. $U/U_{L\max}$. For $U/U_{L\max} > 1$, data are best fitted to $L/L_{\max} = (U/U_{L\max})^{-2.5}$. The value of $\alpha/\alpha_{L\max}$ can be obtained from the slope of L/L_{\max} vs. $U/U_{L\max}$ curve as given in equation (5.5). Figure 5.7 presents the variation of $\alpha/\alpha_{L\max}$ with respect to $U/U_{L\max}$. This plot combines the trend of disturbance growth in all nine sets of data.

Chen and Ritcher [7] carried out numerical analysis on instability of gas-liquid jet by solving dispersion equation (3.3) and presented data as plots of α vs. Mach number, M . These plots are reproduced in Figure 5.8 (a), (b) and (c).





**Figure 5.8: Variation of growth rate with Mach number
for (a) $k=0.5$, (b) $k=1$ & (c) $k=2\pi$**

It is evident from their numerical analysis that the growth rate increases as the Mach number increases in the subsonic region and reaches the maximum point where the Mach number approaches unity.

However, the experimental range of Mach number for present study is 0.001-0.09. The trend of disturbance growth rate illustrated in the numerical analysis [7] in this regime is much lower than that is obtained from the present experimental study. This implies that disturbance generated on the studied jet surface is much stronger than that is predicted by the numerical analysis. Viscous effect of the surrounding liquid, jet turbulence, nozzle roughness and nozzle passage length are some of the factors ignored by the analysis of Chen and Ritcher [7] which may have significant contribution to the growth rate of disturbance.

Chapter 6

Conclusion

The present work is mainly focused on the experimental investigation of submerged air jet with respect to jet velocity, nozzle size and liquid properties. Measured data of jet lengths versus jet velocities are presented here for the first time for gas/liquid systems. It was observed that the jet length goes through a maximum value as the velocity increases. Nozzle sizes, physical properties of liquids also have major impact on the nature of disturbance, on the jet surface as well as the jet break-up length. Reported instability analyses of gas/liquid interface for flowing gas jets in liquids are used to interpret the observations. A criterion to approximate the trend of growth rate with respect to jet velocity is set by U/U_{Lmax} which corresponds to jet length L/L_{max} and growth rate α/α_{Lmax} . For $U/U_{Lmax} < 1$, $\alpha/\alpha_{Lmax} = 1$ and for $U/U_{Lmax} > 1$, α/α_{Lmax} varies as $(U/U_{Lmax})^{3.5}$. Disturbance generated on the studied jet surface is much stronger than that is predicted by the numerical analysis

The present study is a preliminary experimental work on gas/liquid system. The research can be modified and extended in diversified way. The following suggestions can be made for future work on this topic.

Though in the present study viscosity of the liquid was found to have a destabilizing effect on jet break-up length experiments can be done on more liquids with different viscosity and surface tension to single out the effect of liquid properties on jet break-up length. Roughness of nozzle can be measured experimentally. Variation of jet length and air jet stability with nozzle roughness can be analysed to measure the effect of nozzle roughness on growth rate of disturbance. The trend of α is much higher than that of reported numerical analysis. Inclusion of viscosity of liquid, turbulence and nozzle roughness in the theoretical analysis are suggested for better agreement of theory and experimental findings.

Chapter 7

Reference

1. Rayleigh Lord., "Theory of Sound", 2nd edn, vol. II. Dover, 1896.
2. Drazin P. G., Reid W. H., "Hydrodynamic Stability", Cambridge University Press, 1981.
3. Grant R.P., Middleman. S., "Newtonian Jet Stability", A.I.Ch.E., Vol.12, 669, 1966.
4. Koria S.C., "Principles and applications of gas injection in steelmaking practice", Scandinavian, J. Metall., Vol. 22, p271, 1993.
5. Chawla T.C., "The Kelvin-Helmholtz instability of the gas-liquid interface of a sonic gas jet submerged in a liquid", J. Fluid Mech., Vol.67, p513-537, 1975.
6. Chan S.H., Wang, Y.S., Tan, C.C., "The effect of mass transfer on Kelvin-Helmholtz instability at the gas- liquid interface of a sonic reacting and non-reacting gas jet submerged in a liquid", Int. J. Heat Mass Transfer, Vol.37, Issue 7, p1123-1132, 1994.
7. Chen K., Richter H.J., "Instability analysis of the transition from bubbling to jetting in a gas injected into a liquid", Int. J. Multi phase Flow, Vol.23, p699-712, 1997.
8. Maccarthy M. J., Molloy N. A., "Review of Stability of Liquid Jets and the Influence of Nozzle Design", Chem. Engg. J., 7, I-20, 1974.
9. Bogy D. B., "Drop Formation in a Circular Liquid Jet", Ann. Rev. Fluid Mech., 11, 207-227, 1979.
10. Goedde E. F., Yuen M. C., "Experiments on liquid jet instability", J. Fluid Mech., 40, 495-514, 1970.
11. Yakubenko P. A., "Capillary instability of an ideal jet of large but finite length", Eur. J. Mech. B/Fluids., 16 (1), 3947, 1997.
12. Leib S. J., Goldstein M. E., "The generation of capillary instabilities in a liquid jet", J. Fluid Mech., 168, 479-500, 1986.

13. Debler W., Yu D., "The Break-up of Laminar Liquid Jets", Proc. Roy. Soc. Lond. A, 415, 106-120, 1988.
14. Hoyt J. W., Taylor J. J., "Waves on water jets", J. Fluid Mech., 83, 119-227, 1968.
15. Brennen C., "Cavity surface wave patterns and general appearance", J. Fluid Mech., 44, 33, 1970.
16. Hashimoto H., Suzuki T., "Experimental and Theoretical Study of Fine Interfacial Waves on Thin Liquid Sheet", JSME Int. J. Serie. II, 34, No. 3, 277-283, 1991.
17. Lienhard J. H., "Effects of Gravity and Surface Tension Upon Liquid Jets Leaving Poiseuille Tubes", J. Basic Eng., 226, 425-443, 1968.
18. Reitz R., Bracco F., "Mechanism of atomization of a liquid jet", Phys. Fluids 25, 1730-1742, 1982.
19. Lin, S., Reitz, R. "Drop and spray formation from a liquid jet". Annu. Rev. Fluid Mech. 30, 85-105, 1998.
20. Sterling A., Sleicher C., "The instability of capillary jets", J. Fluid Mech. 68, 477-495, 1975.
21. Weber C., "On the breakdown of a fluid jet", Z. Angew. Math. Mech. 11, 136-141, 1931.
22. Gordillo J. M., Perez-Saborid M., "Aerodynamic effects in the break-up of liquid jets: on the first wind-induced break-up regime", J. Fluid Mech. (2005), vol. 541, 1-20, 2005.
23. Liu Z., Liu Z., "Instability of a Viscoelastic Liquid Jet with Axisymmetric and Asymmetric Disturbances", International Journal of Multiphase Flow 34 42-60, 2008.
24. Gulawani S. S. et al., "Submerged Gas Jet into a Liquid Bath: A Review", Ind. Eng. Chem. Res., 46 (10), 3188-3218, 2007.
25. Chawla, T. C., "Equation of Motion of a Liquid-Submerged Sonic Gas Jet Relative to Fission Gas Jet Impingement in Subassemblies of the Liquid Metal Fast Breeder Reactor", Nucl. Sci. Eng. 53, 466, 1974.
26. Chawla, T. C., "Rate of Liquid Entrainment at the Gas-Liquid Interface of a Liquid Submerged Sonic Gas Jet", Nucl. Sci. Eng., 56, I, 1975.

27. Payne G. J., Price R. G., "The transition from jetting to bubbling at a submerged orifice", *Trans. Instn Chem. Engrs* 53, 209, 1975.
28. Ozawa Y., Mori K., "Behavior of gas jets injected into a two-dimensional liquid metal bath", *Trans. I.S.I.J.* 23, 759, 1983.
29. Ozawa Y., Mori K., "Characteristics of jetting observed in gas injection into liquid", *Trans. I.S.I.J.* 23, 764, 1983.
30. McNallen M. J., King T. B., "Fluid dynamics of vertical submerged gas jets in liquid metal processing systems", *Metall. Trans. B* 13B, 165, 1982.
31. Leonard J. W. III., "Coal Preparation", 5th ed., Society for Mining, Metallurgy and Exploration, Littleton, Colorado, 1991.
32. Kendall J. M., "Experiments on annular liquid jet instability and on the formation of liquid shells", *Phys. Fluids* 29, 2086, 1986.
33. Li X., Bhunia A., "Temporal instability of plane gas sheets in a viscous liquid medium", *Phys. Fluids* 8, 103, 1996.
34. Radwan A. E., "Instability of a hollow jet with effects of surface tension and fluid inertia", *J. Phys. Soc. Jpn.* 58, 1225, 1989.
35. Parthasarathya R. N., Chiang Kai-Ming, "Temporal instability of gas jets injected in viscous liquids to three-dimensional disturbances", *Physics of Fluids*, Volume 10, Number 8 August 1998.
36. Lee J.G., Chen L.D., "Linear stability analysis of gas-liquid interface," *AIAA J.* 29, 1589, 1991.
37. Chang D., Russel P. E., "Stability of a liquid adjacent to high-speed gas stream", *Phys. Fluids* 8(6), 1018-1026, 1965.
38. Nachtsheim P. R., "Stability of crosshatched wave patterns in thin liquid films adjacent to supersonic streams", *Phys. Fluids* 13(13), 2432-2447, 1970.
39. Nayfeh H., Saric W. S., "Non-linear Kelvin-Helmholtz instability", *Fluid Mech.* 46, 2099231, 1971.
40. D. D. Craik,, "Wind-generated waves in thin liquid films", *Fluid Mech.* 26, 369-392, 1966.

41. Cho D. H., Armstrong D. R., Bova L., "Experimental Study of Reacting Gas Jets in Liquids", *Heat Release Effects. Chem. Eng. Sci.* 45 (2), 423, 1990.
42. Blaisot JB., Adeline S., "Determination of the growth rate of instability of low velocity free falling jets", *Exp Fluids* 29:247-256, 2000.
43. Blaisot JB., Adeline S., "Instabilities on a free falling jet under an internal flow break-up mode regime", *Int J Multiphase Flow* 29:629-653, 2003.
44. Dumouchel C., Cousin J., Triballier K., "Experimental Analysis of Liquid-Gas Interface at Low Weber Number: Interface Length and Fractal Dimension", *Experiments in Fluids* 39: 651-666, 2005.
45. Rensen J., Roig V., "Experimental study of the unsteady structure of a confined bubble plume", *Int. J. Multiphase Flow* 27, 1431, 2001.
46. Matsumoto O., Sugihara M., Miya K., "Underwater cutting of reactor core internals by CO laser using local-dry-zone creating nozzle", *J. Nucl. Sci. Technol.* 29, 1074, 1992.
47. Bisio G., Rubatto G., "Process improvements in iron and steel industry by analysis of heat and mass transfer", *Energy Convers. Manage.* 43, 205, 2002.
48. Gavigan J. J., Watson E. E., King W.F.III., "Noise generation by gas jets in a turbulent wake", *J. Acoust. Soc. Am.* 56, 1094, 1974.
49. Fabritius T. M. J., Mure P. T., Harkki J. J., "The determination of the minimum and operational gas flow rates for sidewall blowing in the AOD-Converter", *ISIJ Int.* 43, 1177, 2003.
50. Yang Q. X., Gustavsson H., "Effects of gas jet instability on refractory wear; a study by high-speed photography", *Scand. J. Metall.* 21, 15, 1992.
51. Aoki T. et al., "Characteristics of submerged gas jets and a new type bottom blowing tuyere", In: Wraith A.E. (ed) *Injection Phenomena in Extraction and Refining*, New Castle, April 21-22, pp.A1-A36, 1982.
52. Taylor I. F., Wright, J. K., Philp, D. K., "Transient pressure and vibration events resulting from high speed gas injection into liquids", *Can. Inst. Min. Metall.* 27, 293, 1988.

53. Yang Q. X., Gustavsson H., Burstrom E., "Erosion of refractory during gas injection – a cavitation based model", *Scand. J. Metall.* 19, 127, 1990.
54. Qi L. X., Chao Y., Wang B. Y., "Experimental study of underexpanded sonic air jets in water", *Acta Mech. Sin.* 32, 667, 2000.
55. Shi H. H. et al., "The measurement of fluctuating pressures induced by submerged high-speed gas jet", In: *Proceedings of the 4th International Symposium on Advanced Fluid Information and Trans disciplinary Fluid Integration*, Sendai, Japan, November 11–12, pp. 77–81, 2004.
56. Dai Z. et al., "Experimental study on hydrodynamic behaviors of high-speed gas jets in still water", *Acta Mechanica Sinica*, 22:443–448, 2006.
57. Ozawa Y., Mori K., "Characterization of jetting observed in gas injection into liquid", *Trans. ISIJ* 23, 765, 1983.
58. Sundar R., Tan R. B. H., "A model for bubble-to-jet transition at a submerged orifice", *Chemical Engineering Science*, Vol. 54, Issue 18, 4053-4060, 1999.
59. Lockett M. J., "The froth to spray transition on sieve trays", *Chemical Engineering Research and Design*, Vol. 59a, 26-34, 1981.

Appendix A
Physical Properties of Liquids

A.1: Physical Properties of Liquids

Table A-1: Physical Properties of ethanol, water and glycerol

Name of Liquid	Molecular Weight	Boiling Point (C) at 1 atm	Density (gm/cc) at 30C	Surface Tension (dynes/cm) at 30C	Viscosity (cp) at 30C
ethanol	46.07	78.5	0.7893	22.10	1.2
water	18	100	0.998	73.05	1.002
glycerol	-	-	1.261	63.00	1500

Appendix B

Data Obtained for Air/Liquid System at Various Nozzle Size

B.1: Data Obtained for 1mm nozzle size

B.1.1: Variation of Height of the jet with jet velocity for Ethanol

Table B-1: Variation of Height of the jet with velocity of jet in 1mm nozzle

flow rate Q cm^3/s	diameter of the nozzle mm	diameter of the nozzle cm	nozzle cross sectional area cm^2	air velocity U cm/s	Height of the jet L Cm
13.88889	1	0.1	0.00785	1769.285209	6.04
16.66667	1	0.1	0.00785	2123.142251	8.1
27.77778	1	0.1	0.00785	3538.570418	10.75
33.33333	1	0.1	0.00785	4246.284501	12.7
38.88889	1	0.1	0.00785	4953.998585	13
41.66667	1	0.1	0.00785	5307.855626	13

B.1.2: Variation of Height of the jet with jet velocity for Water

Table B-2: Variation of Height of the jet with velocity of jet in 1mm nozzle for water

flow rate Q cm^3/s	diameter of the nozzle mm	diameter of the nozzle cm	nozzle cross sectional area cm^2	air velocity U cm/s	Height of the jet L Cm
16.66667	1	0.1	0.00785	2123.142251	5.65
19.44444	1	0.1	0.00785	2476.999292	7.7
22.22222	1	0.1	0.00785	2830.856334	9.15
27.77778	1	0.1	0.00785	3538.570418	9.8
30.55556	1	0.1	0.00785	3892.427459	10.6
33.33333	1	0.1	0.00785	4246.284501	11.58
36.11111	1	0.1	0.00785	4600.141543	12.3

B.1.3: Variation of Height of the jet with jet velocity for Glycerol

Table B-3: Variation of Height of the jet with velocity of jet in 1mm nozzle

flow rate Q cm^3/s	diameter of the nozzle mm	diameter of the nozzle cm	nozzle cross sectional area cm^2	air velocity U cm/s	Height of the jet L Cm
15.27778	1	0.1	0.00785	1946.21373	1.1
17.36111	1	0.1	0.00785	2211.606511	1.67
19.44444	1	0.1	0.00785	2476.999292	1.83
21.52778	1	0.1	0.00785	2742.392074	2
23.61111	1	0.1	0.00785	3007.784855	2.45

B.1.4: Variation of Height of the jet with Reynolds number for Ethanol

Table B-4: Variation of Height of the jet with Reynolds number in 1mm nozzle

air velocity U , cm/s	Density of Ethanol ρ , g/cc	Viscosity of Ethanol μ , cp	Viscosity of Ethanol μ , poise	Reynolds number Re	Height of the jet L , cm
1769.285209	0.7893	1.2	0.012	11637.47346	6.04
2123.142251	0.7893	1.2	0.012	13964.96815	8.1
3538.570418	0.7893	1.2	0.012	23274.94692	10.75
4246.284501	0.7893	1.2	0.012	27929.93631	12.7
4953.998585	0.7893	1.2	0.012	32584.92569	13
5307.855626	0.7893	1.2	0.012	34912.42038	13

B.1.5: Variation of Height of the jet with Reynolds number for Water

Table B-5: Variation of Height of the jet with Reynolds number in 1mm nozzle

air velocity U , cm/s	Density of Water ρ , g/cc	Viscosity of Water μ , cp	Viscosity of Water μ , poise	Reynolds number Re	Height of the jet L , cm
2123.142251	0.998	1.002	0.01002	21146.66633	5.65
2476.999292	0.998	1.002	0.01002	24671.11072	7.7
2830.856334	0.998	1.002	0.01002	28195.5551	9.15
3538.570418	0.998	1.002	0.01002	35244.44388	9.8
3892.427459	0.998	1.002	0.01002	38768.88827	10.6
4246.284501	0.998	1.002	0.01002	42293.33266	11.58
4600.141543	0.998	1.002	0.01002	45817.77704	12.3

B.1.6: Variation of Height of the jet with Reynolds number for Glycerol

Table B-5: Variation of Height of the jet with Reynolds number in 1mm nozzle

air velocity U, cm/s	Density of Glycerol ρ , g/cc	Viscosity of Glycerol μ , cp	Viscosity of Glycerol μ , poise	Reynolds number Re	Height of the jet L, cm
1946.21373	1.261	1500	15	16.36117009	1.1
2211.606511	1.261	1500	15	18.59223874	1.67
2476.999292	1.261	1500	15	20.82330738	1.83
2742.392074	1.261	1500	15	23.05437603	2
3007.784855	1.261	1500	15	25.28544468	2.45

B.1.7: Variation of Height of the jet with Weber No. and Mach No. for Ethanol

Table B-7: Variation of Height of the jet with Weber no. and Mach no. in 1mm

air velocity U, cm/s	density, ρ g/cc	surface tension, σ dynes/cm	Weber number We	Mach number M	Height of the jet, L cm
38.97103984	0.7893	22.1	11180.1	0.053291723	6.04
32.16882198	0.7893	22.1	16099.34	0.063950068	8.1
38.25481532	0.7893	22.1	44720.38	0.106583446	10.75
37.91325447	0.7893	22.1	64397.35	0.127900136	12.7
43.07824856	0.7893	22.1	87651.95	0.149216825	13
46.15526632	0.7893	22.1	100620.9	0.159875169	13

B.1.8: Variation of Height of the jet with Weber no. and Mach number for Water

Table B-8: Variation of Height of the jet with Weber no. and Mach no. in 1mm

air velocity U, cm/s	density, ρ g/cc	surface tension, σ dynes/cm	Weber number We	Mach number M	Height of the jet, L cm
37.57773895	0.998	73.05	6158.409	0.063950068	5.65
32.16882198	0.998	73.05	8382.278	0.074608412	7.7
30.93832059	0.998	73.05	10948.28	0.085266757	9.15
36.1078614	0.998	73.05	17106.69	0.106583446	9.8
36.72101377	0.998	73.05	20699.1	0.117241791	10.6
36.65857123	0.998	73.05	24633.63	0.127900136	11.58
37.39952474	0.998	73.05	28910.31	0.13855848	12.3

B.1.9: Variation of Height of the jet with Weber No. and Mach No. for Glycerol

Table B-9: Variation of Height of the jet with Weber no. and Mach no. in 1mm

air velocity U, cm/s	density, ρ g/cc	surface tension, σ dynes/cm	Weber number We	Mach number M	Height of the jet, L Cm
176.928521	1.261	63	7581.508	0.0586209	1.1
132.696125	1.261	63	9790.171	0.06661465	1.67
135.111509	1.261	63	12280.79	0.07460841	1.83
137.119604	1.261	63	15053.37	0.08260217	2
122.766729	1.261	63	18107.9	0.09059593	2.45

B.2: Data Obtained for 4mm nozzle size

B.2.1: Variation of Height of the jet with jet velocity for Ethanol

Table B-10: Variation of Height of the jet with velocity of jet in 4mm nozzle

flow rate Q cm ³ /s	diameter of the nozzle mm	diameter of the nozzle cm	nozzle cross sectional area cm ²	air velocity U cm/s	Height of the jet L Cm
10.22222222	4	0.4	0.1256	81.3871196	2.58889
22.72222222	4	0.4	0.1256	180.9094126	3.7375
38	4	0.4	0.1256	302.5477707	4.4
51.88888889	4	0.4	0.1256	413.1280962	5.05
61.61111111	4	0.4	0.1256	490.5343241	3.771428571
69.94444444	4	0.4	0.1256	556.8825195	2.5090909

B.2.2: Variation of Height of the jet with jet velocity for Water

Table B-11: Variation of Height of the jet with velocity of jet in 4mm nozzle for water

flow rate Q cm^3/s	diameter of the nozzle mm	diameter of the nozzle cm	nozzle cross sectional area cm^2	air velocity U cm/s	Height of the jet L Cm
11.11111	4	0.4	0.1256	88.4642604	0.95
16.66667	4	0.4	0.1256	132.696391	1.6125
22.22222	4	0.4	0.1256	176.928521	2.525
27.77778	4	0.4	0.1256	221.160651	2.766667
33.33333	4	0.4	0.1256	265.392781	3.96667
38.88889	4	0.4	0.1256	309.624912	4.83333
44.44444	4	0.4	0.1256	353.857042	4.96
50	4	0.4	0.1256	398.089172	4.2
62.5	4	0.4	0.1256	497.611465	2.4444
72.22222	4	0.4	0.1256	575.017693	2.2625
81.94444	4	0.4	0.1256	652.423921	0.8857
91.66667	4	0.4	0.1256	729.830149	0.5857

B.2.3: Variation of Height of the jet with jet velocity for Glycerol

Table B-12: Variation of Height of the jet with velocity of jet in 4mm nozzle

flow rate Q cm^3/s	diameter of the nozzle mm	diameter of the nozzle cm	nozzle cross sectional area cm^2	air velocity U cm/s	Height of the jet L Cm
10.41667	4	0.4	0.1256	82.9352442	0.41275
13.88889	4	0.4	0.1256	110.580326	0.725714322
15.27778	4	0.4	0.1256	121.638358	0.873125
17.36111	4	0.4	0.1256	138.225407	1.36525
22.22222	4	0.4	0.1256	176.928521	1.5875
24.30556	4	0.4	0.1256	193.51557	1.666875
27.08333	4	0.4	0.1256	215.631635	2.0955
29.86111	4	0.4	0.1256	237.7477	2.06375
31.25	4	0.4	0.1256	248.805732	1.799166582

B.2.4: Variation of Height of the jet with Reynolds number for Ethanol

Table B-13: Variation of Height of the jet with Reynolds number in 4mm nozzle

air velocity U, cm/s	Density of Ethanol ρ , g/cc	Viscosity of Ethanol μ , cp	Viscosity of Ethanol μ , poise	Reynolds number Re	Height of the jet L, cm
81.3871196	0.7893	1.2	0.012	6206.652512	2.58889
180.909412	0.7893	1.2	0.012	9697.894551	3.7375
302.547770	0.7893	1.2	0.012	13964.96815	4.4
413.128096	0.7893	1.2	0.012	17844.12597	5.05
490.534324	0.7893	1.2	0.012	20559.53645	3.771428571
556.882519	0.7893	1.2	0.012	22887.03114	2.5090909

B.2.5: Variation of Height of the jet with Reynolds number for Water

Table B-14: Variation of Height of the jet with Reynolds number in 4mm nozzle

air velocity U, cm/s	Density of Water ρ , g/cc	Viscosity of Water μ , cp	Viscosity of Water μ , poise	Reynolds number Re	Height of the jet L, cm
88.4642604	0.998	1.002	0.01002	4699.259184	0.95
132.696391	0.998	1.002	0.01002	7048.888776	1.6125
176.928521	0.998	1.002	0.01002	9398.518368	2.525
221.160651	0.998	1.002	0.01002	11748.14796	2.766667
265.392781	0.998	1.002	0.01002	14097.77755	3.96667
309.624912	0.998	1.002	0.01002	16447.40714	4.83333
353.857042	0.998	1.002	0.01002	18797.03674	4.96
398.089172	0.998	1.002	0.01002	21146.66633	4.2
497.611465	0.998	1.002	0.01002	26433.33291	2.4444
575.017693	0.998	1.002	0.01002	30545.1847	2.2625
652.423921	0.998	1.002	0.01002	34657.03648	0.8857
729.830149	0.998	1.002	0.01002	38768.88827	0.5857

B.2.6: Variation of Height of the jet with Reynolds number for Glycerol

Table B-15: Variation of Height of the jet with Reynolds number in 4mm nozzle

air velocity U, cm/s	Density of Glycerol ρ , g/cc	Viscosity of Glycerol M, cp	Viscosity of Glycerol μ , poise	Reynolds number Re	Height of the jet L, cm
82.9352442	1.261	1500	15	3.718447747	0.41275
110.580326	1.261	1500	15	4.957930329	0.725714322
121.638358	1.261	1500	15	5.453723362	0.873125
138.225407	1.261	1500	15	6.197412912	1.36525
176.928521	1.261	1500	15	7.932688527	1.5875
193.51557	1.261	1500	15	8.676378077	1.666875
215.631635	1.261	1500	15	9.667964142	2.0955
237.7477	1.261	1500	15	10.65955021	2.06375
248.805732	1.261	1500	15	11.15534324	1.799166582

B.2.7: Variation of Height of the jet with Weber No. and Mach No. for Ethanol

Table B-16: Variation of Height of the jet with Weber no. and Mach no. in 4mm

air velocity U, cm/s	Density ρ g/cc	surface tension, σ dynes/cm	Weber number We	Mach number M	Height of the jet, L Cm
314.539593	0.7893	22.1	1060.039	0.002451	2.58889
491.468114	0.7893	22.1	2587.985	0.005449	3.7375
707.714084	0.7893	22.1	5366.446	0.009113	4.4
904.301329	0.7893	22.1	8761.882	0.012444	5.05
1041.9124	0.7893	22.1	11631.44	0.014775	3.771428571
1159.86475	0.7893	22.1	14414.04	0.016774	2.5090909

B.2.8: Variation of Height of the jet with Weber no. and Mach number for Water

Table B-17: Variation of Height of the jet with Weber no. and Mach no. in 4mm

air velocity U, cm/s	Density ρ g/cc	surface tension, σ dynes/cm	Weber number We	Mach number M	Height of the jet, L Cm
88.4642604	0.998	73.05	101.373	0.002665	0.95
132.696391	0.998	73.05	228.0892	0.003997	1.6125
176.928521	0.998	73.05	405.4919	0.005329	2.525
221.160651	0.998	73.05	633.5811	0.006661	2.766667
265.392781	0.998	73.05	912.3568	0.007994	3.96667
309.624912	0.998	73.05	1241.819	0.009326	4.83333
353.857042	0.998	73.05	1621.968	0.010658	4.96
398.089172	0.998	73.05	2052.803	0.011991	4.2
497.611465	0.998	73.05	3207.505	0.014988	2.4444
575.017693	0.998	73.05	4283.009	0.01732	2.2625
652.423921	0.998	73.05	5513.74	0.019651	0.8857
729.830149	0.998	73.05	6899.699	0.021983	0.5857

B.2.9: Variation of Height of the jet with Weber No. and Mach No. for Glycerol

Table B-18: Variation of Height of the jet with Weber no. and Mach no. in 4mm

air velocity U, cm/s	Density ρ g/cc	surface tension, σ dynes/cm	Weber number We	Mach number M	Height of the jet, L Cm
82.9352442	1.261	63	130.5356	0.002498	0.41275
110.580326	1.261	63	232.0633	0.003331	0.725714322
121.638358	1.261	63	280.7966	0.003664	0.873125
138.225407	1.261	63	362.5989	0.004163	1.36525
176.928521	1.261	63	594.0821	0.005329	1.5875
193.51557	1.261	63	710.6939	0.005829	1.666875
215.631635	1.261	63	882.4207	0.006495	2.0955
237.7477	1.261	63	1072.713	0.007161	2.06375
248.805732	1.261	63	1174.82	0.007494	1.799166582

B.3: Data Obtained for 6mm nozzle size

B.3.1: Variation of Height of the jet with jet velocity for Ethanol

Table B-19: Variation of Height of the jet with velocity of jet in 6mm nozzle

flow rate Q cm^3/s	diameter of the nozzle mm	diameter of the nozzle cm	nozzle cross sectional area cm^2	air velocity U cm/s	Height of the jet, L Cm
7.222222222	6	0.6	0.2826	25.5563419	1.398765444
19.72222222	6	0.6	0.2826	69.78847212	2.5484375
35	6	0.6	0.2826	123.8499646	3.00625
48.88888889	6	0.6	0.2826	172.996776	3.65625
58.61111111	6	0.6	0.2826	207.3995439	2.174489857
66.94444444	6	0.6	0.2826	236.8876307	0.914462818

B.3.2: Variation of Height of the jet with jet velocity for Water

Table B-20: Variation of Height of the jet with velocity of jet in 6mm nozzle for water

flow rate Q cm^3/s	diameter of the nozzle mm	diameter of the nozzle Cm	nozzle cross sectional area cm^2	air velocity U cm/s	Height of the jet, L Cm
13.1944444	6	0.6	0.2826	46.689470	0.3175
19.4444444	6	0.6	0.2826	68.805535	2.143125
22.9166666	6	0.6	0.2826	81.092238	2.8178125
30.5555555	6	0.6	0.2826	108.12298	3.01625
34.7222222	6	0.6	0.2826	122.86702	3.175
37.5	6	0.6	0.2826	132.69639	3.5151797
40.9722222	6	0.6	0.2826	144.98309	3.095625
44.4444444	6	0.6	0.2826	157.26979	2.2225
47.9166666	6	0.6	0.2826	169.55649	2.2225
51.3888888	6	0.6	0.2826	181.84320	1.984375
54.8611111	6	0.6	0.2826	194.12990	1.42875
64.5833333	6	0.6	0.2826	228.53267	0.9525
79.16666667	6	0.6	0.2826	280.136825	0.9525

B.3.3: Variation of Height of the jet with jet velocity for Glycerol

Table B-21: Variation of Height of the jet with velocity of jet in 6mm nozzle

flow rate Q cm^3/s	diameter of the nozzle mm	diameter of the nozzle cm	nozzle cross sectional area cm^2	air velocity U cm/s	Height of the jet, L Cm
15.277777	6	0.6	0.2826	54.06149	0.9525
17.083333	6	0.6	0.2826	60.450578	1.217083
19.444444	6	0.6	0.2826	68.80553	1.230313
21.527777	6	0.6	0.2826	76.17755	1.23825
23.611111	6	0.6	0.2826	83.54958	1.397
25.694444	6	0.6	0.2826	90.921601	1.5875
28.194444	6	0.6	0.2826	99.76802	1.690221
30.555555	6	0.6	0.2826	108.123	1.322917
32.638889	6	0.6	0.2826	115.495	1.222375
34.722222	6	0.6	0.2826	122.867	1.058333
36.805555	6	0.6	0.2826	130.23905	1.058333
39.58333	6	0.6	0.2826	140.0684	1.021953

B.3.4: Variation of Height of the jet with Reynolds number for Ethanol

Table B-22: Variation of Height of the jet with Reynolds number in 6mm nozzle

air velocity U cm/s	Density of Ethanol ρ , g/cc	Viscosity of Ethanol M , cp	Viscosity of Ethanol μ , poise	Reynolds number Re	Height of the jet, L Cm
25.5563419	0.7893	1.2	0.012	3103.326256	1.398765444
69.78847212	0.7893	1.2	0.012	4848.947275	2.5484375
123.8499646	0.7893	1.2	0.012	6982.484076	3.00625
172.996776	0.7893	1.2	0.012	8922.062987	3.65625
207.3995439	0.7893	1.2	0.012	10279.76822	2.174489857
236.8876307	0.7893	1.2	0.012	11443.51557	0.914462818

B.3.5: Variation of Height of the jet with Reynolds number for Water

Table B-23: Variation of Height of the jet with Reynolds number in 6mm nozzle

air velocity U cm/s	Density of Water ρ , g/cc	Viscosity of Water M, cp	Viscosity of Water μ , poise	Reynolds number Re	Height of the jet L Cm
46.6894708	0.998	1.002	0.01002	2790.18514	0.3175
68.8055359	0.998	1.002	0.01002	4111.851786	2.143125
81.0922387	0.998	1.002	0.01002	4846.111033	2.8178125
108.122985	0.998	1.002	0.01002	6461.481378	3.01625
122.867028	0.998	1.002	0.01002	7342.592475	3.175
132.696391	0.998	1.002	0.01002	7929.999873	3.51517966
144.983093	0.998	1.002	0.01002	8664.25912	3.095625
157.269796	0.998	1.002	0.01002	9398.518368	2.2225
169.556499	0.998	1.002	0.01002	10132.77762	2.2225
181.843202	0.998	1.002	0.01002	10867.03686	1.984375
194.129905	0.998	1.002	0.01002	11601.29611	1.42875
228.532673	0.998	1.002	0.01002	13657.222	0.9525
280.136825	0.998	1.002	0.01002	16741.11084	0.9525

B.3.6: Variation of Height of the jet with Reynolds number for Glycerol

Table B-24: Variation of Height of the jet with Reynolds number in 6mm nozzle

air velocity U cm/s	Density of glycerol ρ , g/cc	Viscosity of glycerol μ , cp	Viscosity of glycerol μ , poise	Reynolds number Re	Height of the jet, L Cm
54.06149	1.261	1500	15	2.7268616	0.9525
60.450578	1.261	1500	15	3.0491271	1.217083
68.80553	1.261	1500	15	3.4705512	1.230313
76.17755	1.261	1500	15	3.842396	1.23825
83.54958	1.261	1500	15	4.21424078	1.397
90.921601	1.261	1500	15	4.5860856	1.5875
99.768	1.261	1500	15	5.0323	1.690221
108.123	1.261	1500	15	5.453723	1.322917
115.495	1.261	1500	15	5.825568	1.222375
122.867	1.261	1500	15	6.197413	1.058333
130.23905	1.261	1500	15	6.569258	1.058333
140.0684	1.261	1500	15	7.06505	1.021953

B.3.7: Variation of Height of the jet with Weber No. and Mach No. for Ethanol

Table B-25: Variation of Height of the jet with Weber no. and Mach no. in 6mm

air velocity U, cm/s	Density, ρ g/cc	surface tension, σ , dynes/cm	Weber number, We	Mach number, M	Height of the jet, L cm
25.5563419	0.7893	22.1	132.5048	0.00076977	1.398765444
69.78847212	0.7893	22.1	323.4981	0.00210206	2.5484375
123.8499646	0.7893	22.1	670.8057	0.00373042	3.00625
172.996776	0.7893	22.1	1095.235	0.00521075	3.65625
207.3995439	0.7893	22.1	1453.93	0.00624697	2.174489857
236.8876307	0.7893	22.1	1801.755	0.00713517	0.914462818

**B.3.8: Variation of Height of the jet with Weber no. and Mach number for
Water**

Table B-26: Variation of Height of the jet with Weber no. and Mach no. in 6mm

Air velocity U, cm/s	Density, ρ g/cc	surface tension, σ , dynes/cm	Weber number, We	Mach number, M	Height of the jet, L cm
46.68947079	0.998	73.05	17.86897	0.00140631	0.3175
68.8055359	0.998	73.05	38.80684	0.00207246	2.143125
81.09223874	0.998	73.05	53.9039	0.00244254	2.8178125
108.122985	0.998	73.05	95.82915	0.00325672	3.01625
122.8670284	0.998	73.05	123.7463	0.00370081	3.175
132.6963907	0.998	73.05	144.3377	0.00399688	3.51517966
144.9830935	0.998	73.05	172.3044	0.00436696	3.095625
157.2697963	0.998	73.05	202.746	0.00473704	2.2225
169.5564992	0.998	73.05	235.6625	0.00510712	2.2225
181.843202	0.998	73.05	271.0539	0.0054772	1.984375
194.1299049	0.998	73.05	308.9203	0.00584729	1.42875
228.5326728	0.998	73.05	428.1128	0.00688351	0.9525
280.1368247	0.998	73.05	643.2829	0.00843786	0.9525

107210

B.3.9: Variation of Height of the jet with Weber No. and Mach No. for Glycerol

Table B-27: Variation of Height of the jet with Weber no. and Mach no. in 6mm

air velocity U, cm/s	Density, ρ g/cc	surface tension, σ , dynes/cm	Weber number, We	Mach number, M	Height of the jet, L cm
54.06149249	1.261	63	35.09957	0.00162836	0.9525
60.45057797	1.261	63	43.88607	0.0018208	1.217083
68.8055359	1.261	63	56.85551	0.00207246	1.230313
76.1775576	1.261	63	69.69151	0.0022945	1.23825
83.5495793	1.261	63	83.83287	0.00251655	1.397
90.92160101	1.261	63	99.27958	0.0027386	1.5875
99.76802705	1.261	63	119.5387	0.00300506	1.690221
108.122985	1.261	63	140.3983	0.00325672	1.322917
115.4950067	1.261	63	160.1962	0.00347877	1.222375
122.8670284	1.261	63	181.2995	0.00370081	1.058333
130.2390501	1.261	63	203.7081	0.00392286	1.058333
140.0684124	1.261	63	235.6168	0.00421893	1.021953

Different Plots for Air/Liquid System at Various Nozzle Size

C.1 Variation of jet length with flow rate

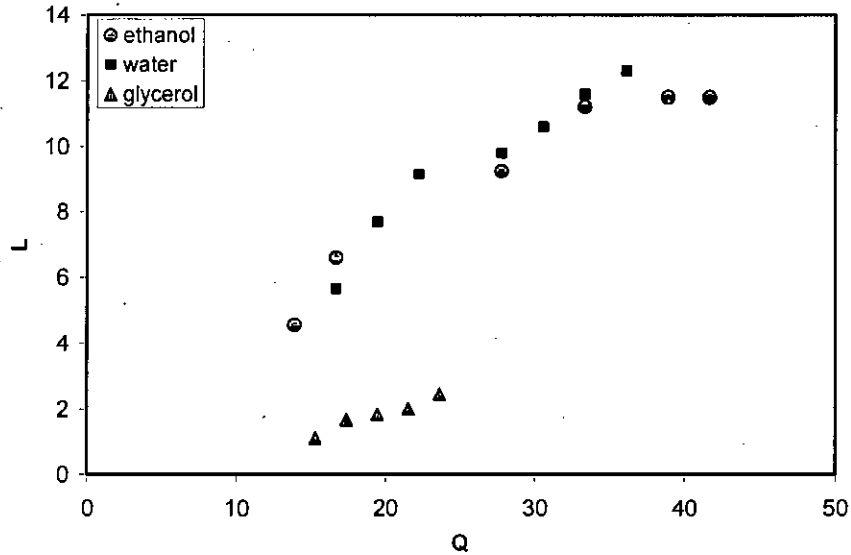


Figure C.1: Variation of jet length with flow rate for 1mm

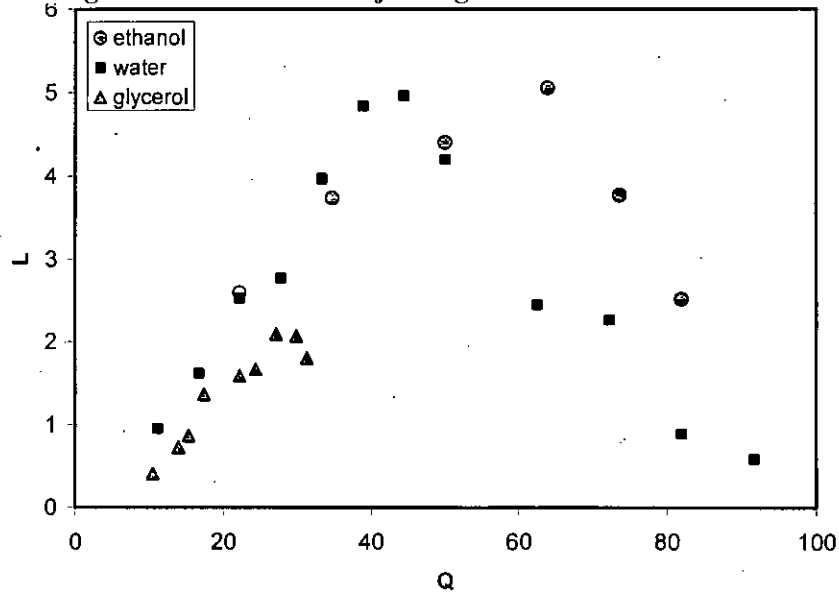


Figure C.2: Variation of jet length with flow rate for 3mm

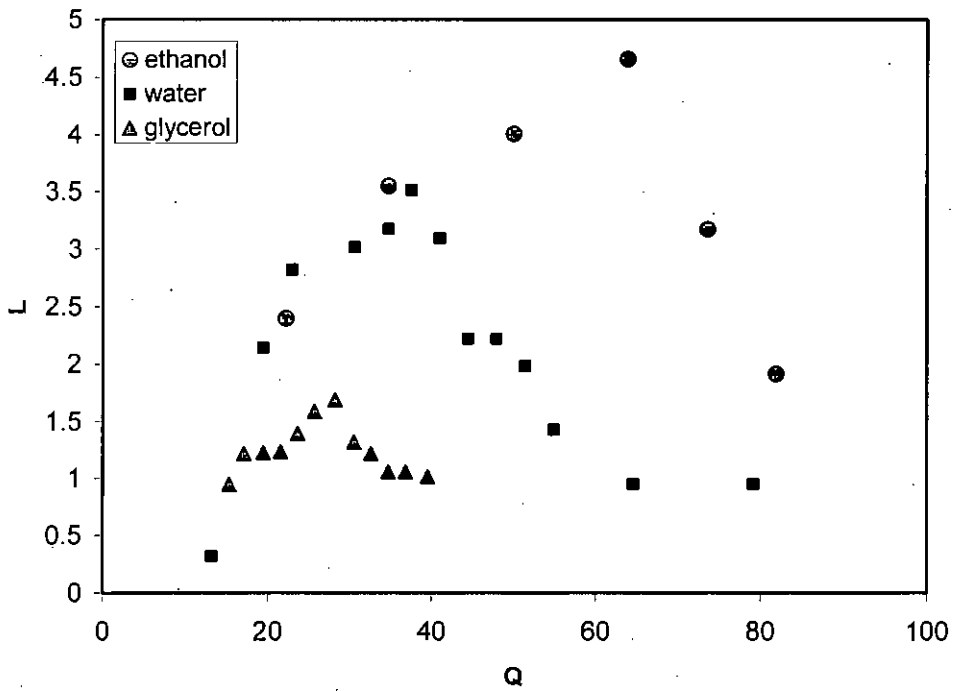


Figure C.3: Variation of jet length with flow rate for 6mm

C.2: Variation of jet length with Reynolds Number

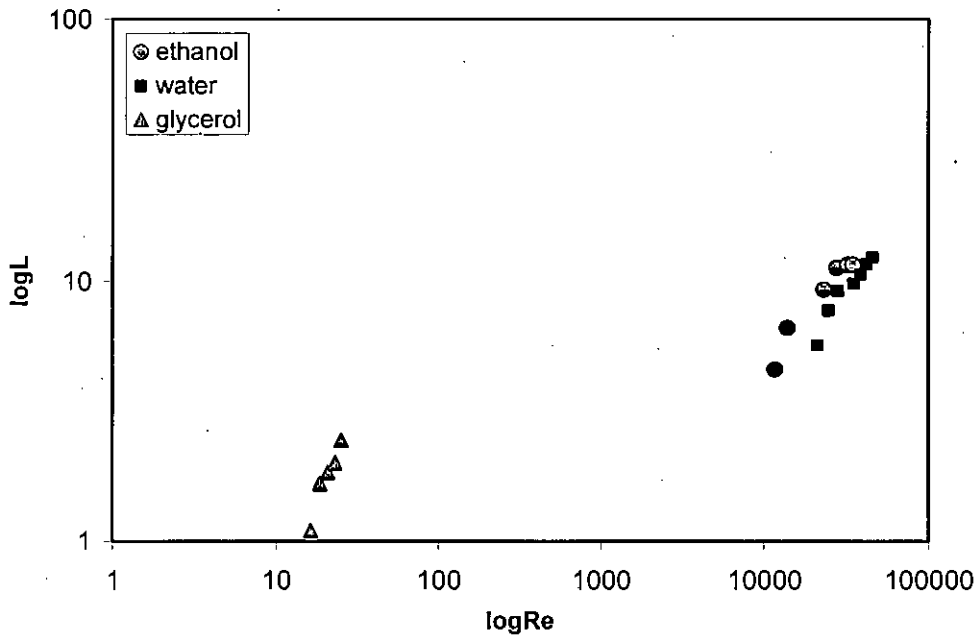


Figure C.4: Variation of jet length with Reynolds Number for 1mm in logarithmic coordinate

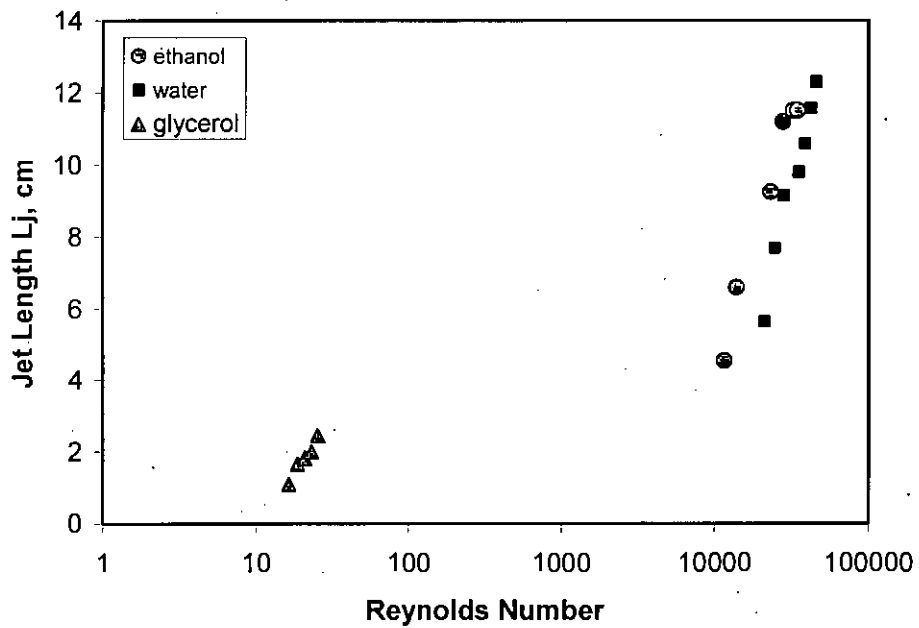


Figure C.5: Variation of jet length with Reynolds Number for 1mm in semi logarithmic coordinate

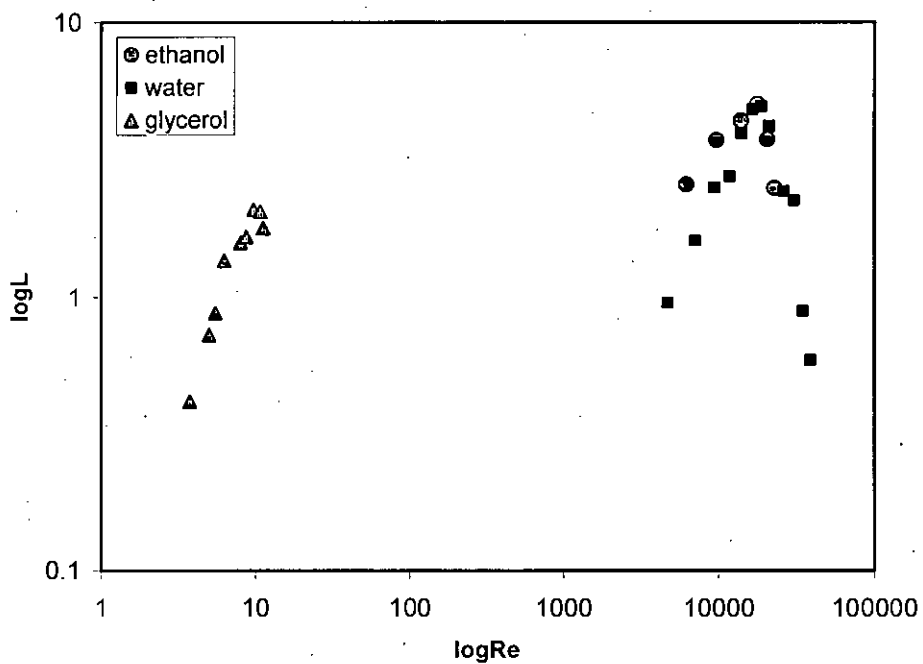


Figure C.6: Variation of jet length with Reynolds Number for 3mm in logarithmic coordinate

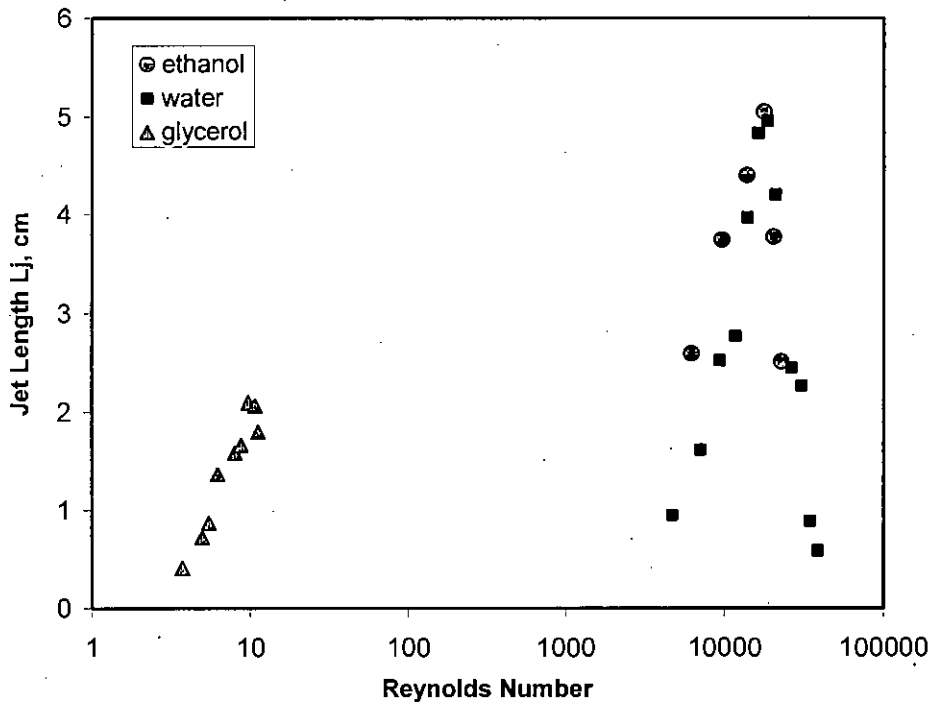


Figure C.7: Variation of jet length with Reynolds Number for 3mm in semi logarithmic coordinate

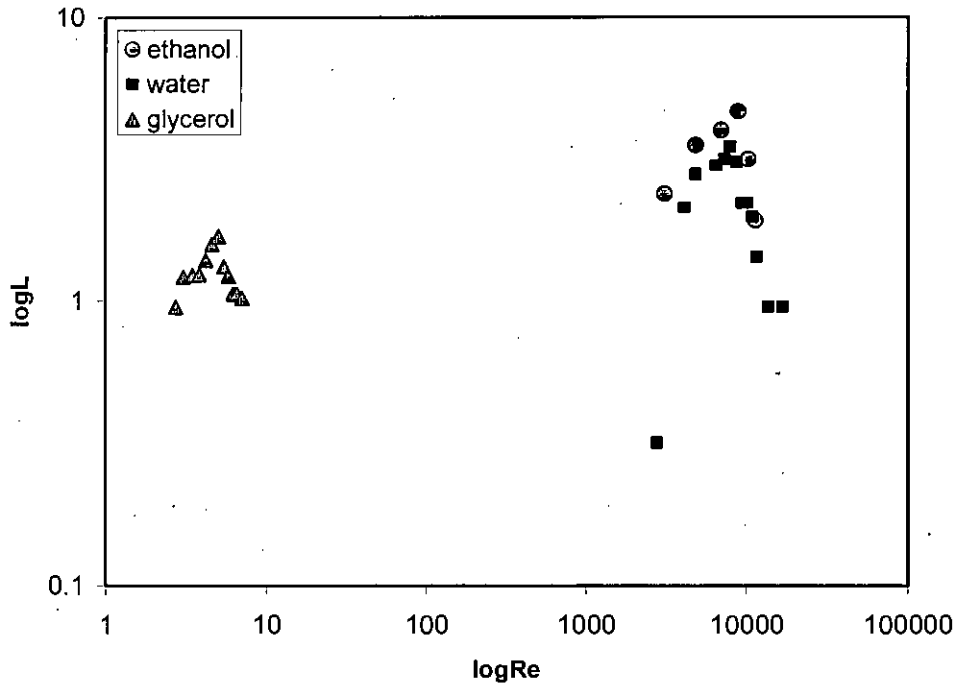


Figure C.8: Variation of jet length with Reynolds Number for 6mm in logarithmic coordinate

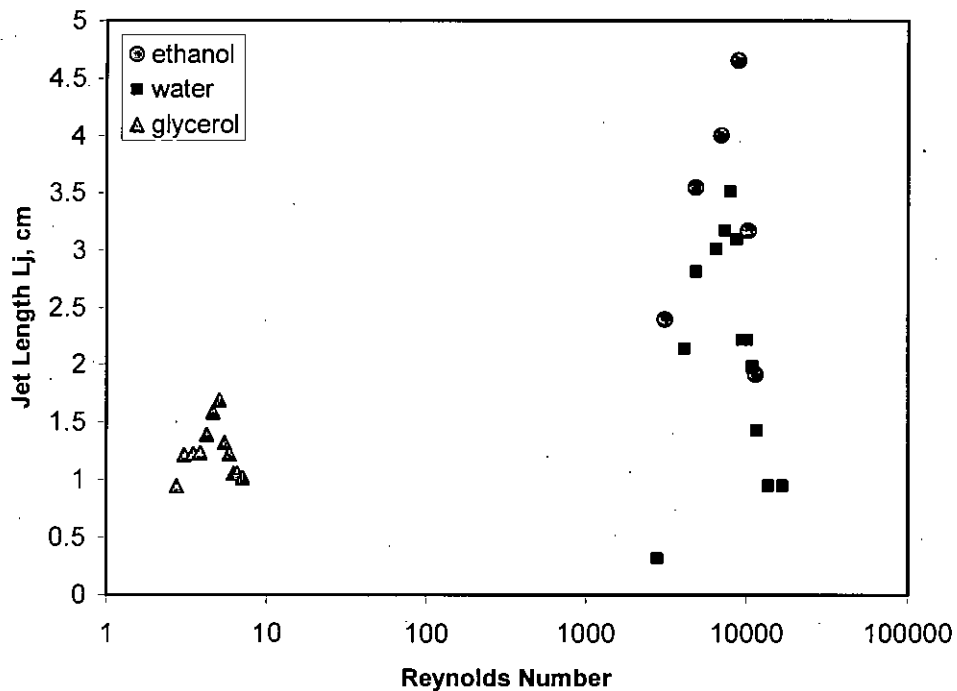


Figure C.9: Variation of jet length with Reynolds Number for 6mm in semi logarithmic coordinate

C.3: Variation of jet length with Weber Number

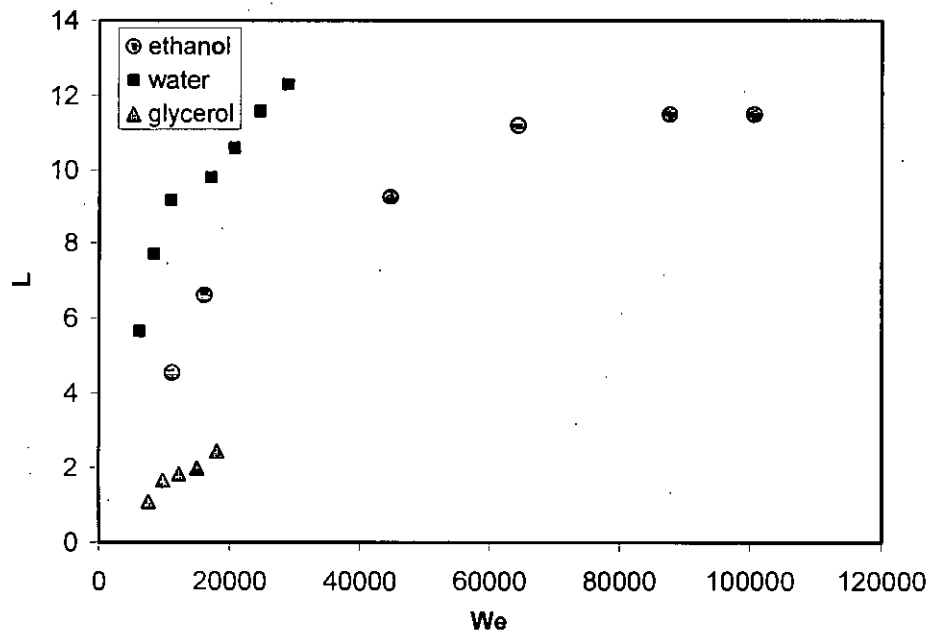


Figure C.10: Variation of jet length with Weber Number for 1mm

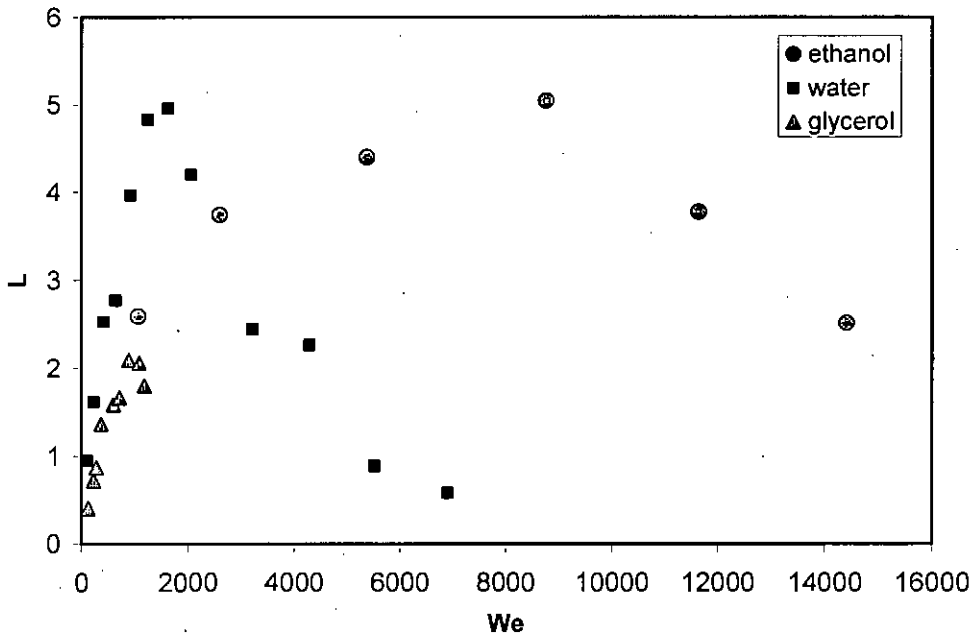


Figure C.11: Variation of jet length with Weber Number for 3mm

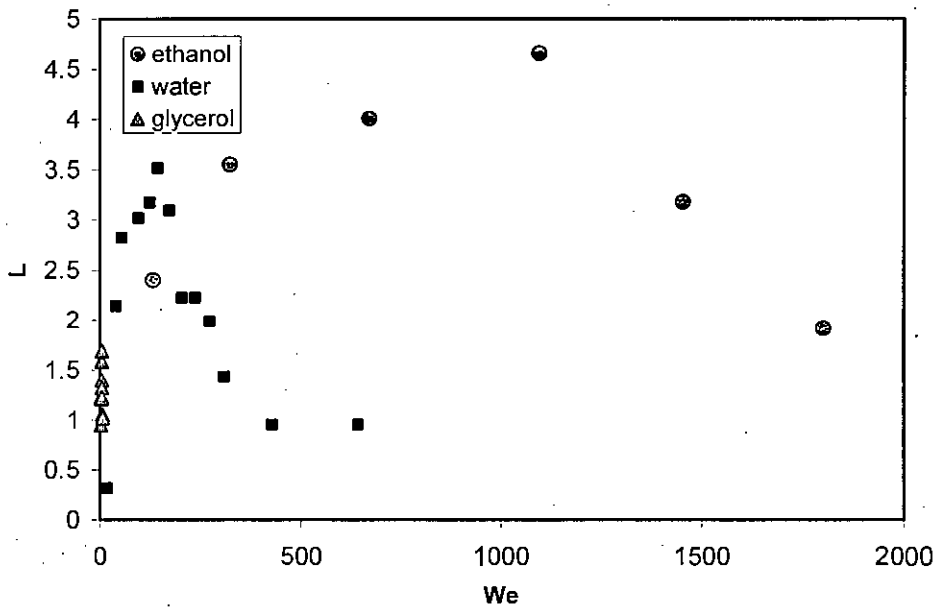


Figure C.12: Variation of jet length with Weber Number for 6mm

C.4: Variation of L/L_{max} ratio with Reynolds Number

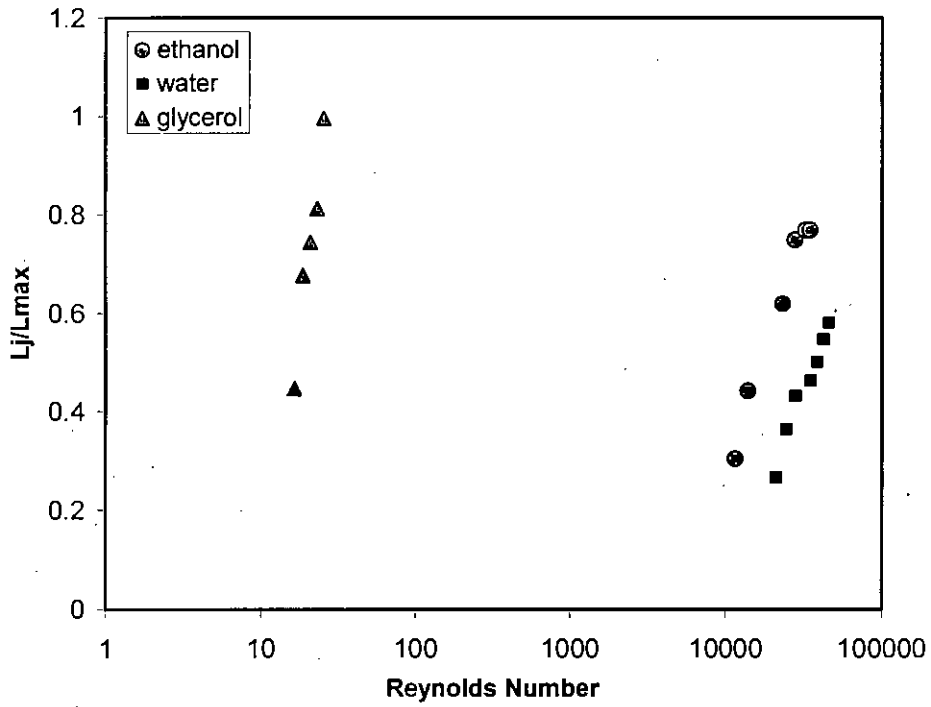


Figure C.13: Variation of L/L_{max} ratio with Reynolds Number for 1mm in semi logarithmic coordinate

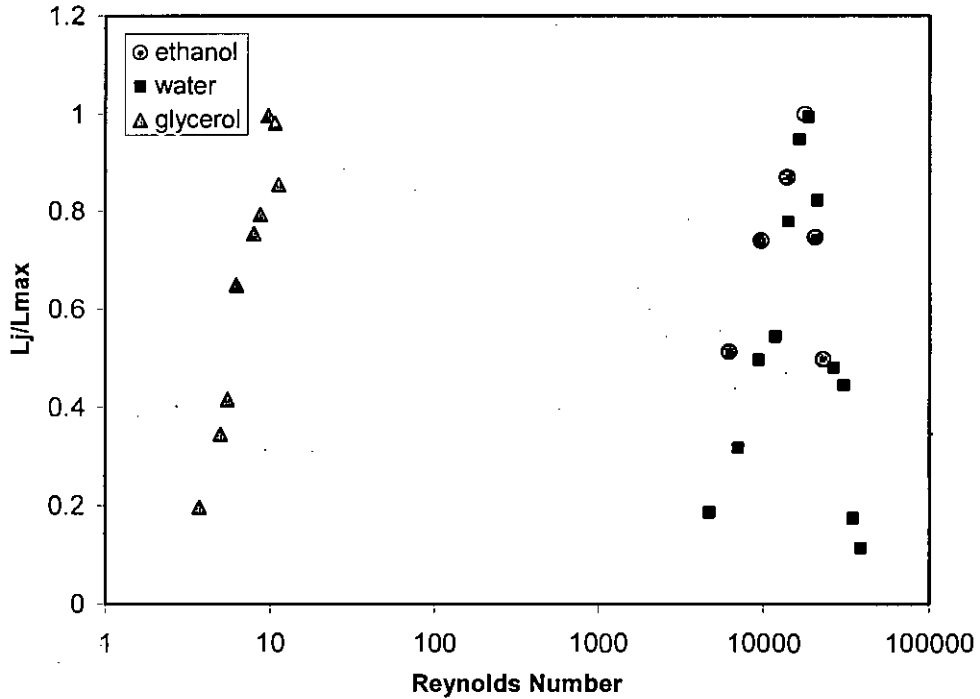


Figure C.14: Variation of L/L_{max} ratio with Reynolds Number for 3mm in semi logarithmic coordinate

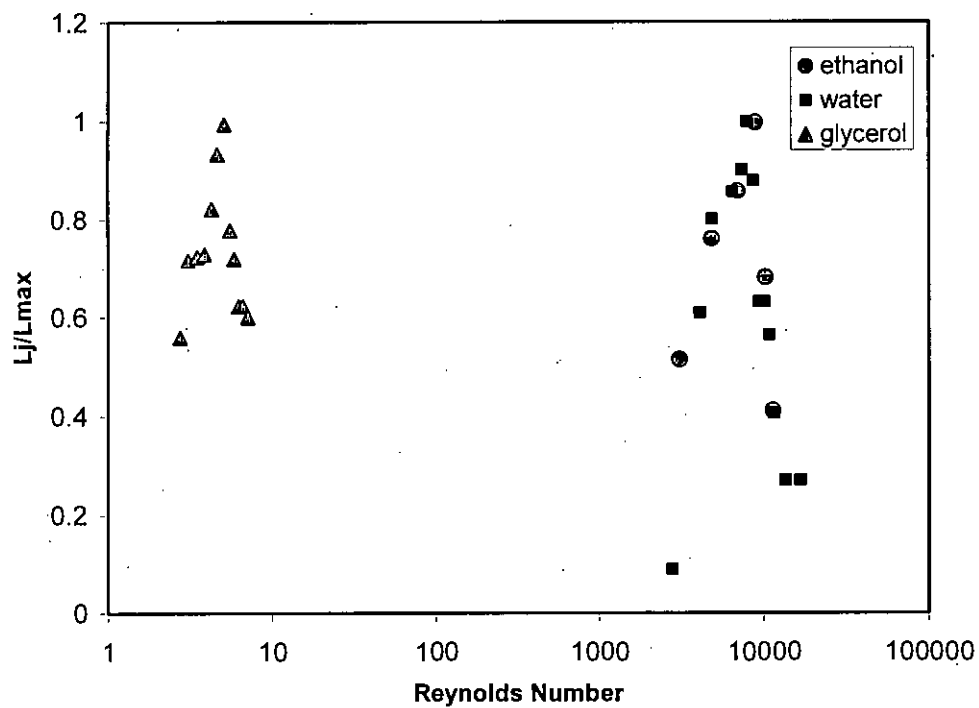


Figure C.15: Variation of L/L_{max} ratio with Reynolds Number for 6mm in semi logarithmic coordinate

